

Supporting Information

Catalyst Free Removal of Trithiocarbonate RAFT CTAs from Poly(vinylpyridine)s Using Tris(trimethylsilyl)silane and Light

*Brandon A. Fultz, Drake Beery, Brianna M. Coia, Kenneth Hanson, and Justin G. Kennemur**

Department of Chemistry & Biochemistry, Florida State University, Tallahassee, FL 32306-4390, United States.

Table of Contents:

I. EXPERIMENTAL

| | |
|-------------------|-------|
| Materials | p. S2 |
| Characterizations | p. S3 |
| Synthesis | p. S4 |

II. ADDITIONAL DATA AND FIGURES

p. S6

| | |
|-------------|---|
| Figure S1. | ¹ H NMR of CDPA. |
| Figure S2. | UV-Vis spectrum of CDPA. |
| Figure S3. | Kinetic evaluation of PMMA-TTC RAFT removal using TTMSS. |
| Figure S4. | Stacked ¹ H NMR of PMMA-TTC and PMMA-H. |
| Figure S5. | ¹ H NMR of PMMA-H with olefin region inset SEC trace of PMMA-TTC. |
| Figure S6. | Kinetic evaluation of TTC RAFT removal using EPHP. |
| Figure S7. | ¹ H NMR of PMMA-H post RAFT removal using EPHP |
| Figure S8. | SEC trace of PMMA-TTC and PMMA-H after RAFT removal using EPHP. |
| Figure S9. | Image of P2VP-TTC and P2VP-H before and after RAFT removal using UV |
| Figure S10. | Stacked ¹ H NMR of PMMA-TTC and PMMA-H. |
| Figure S11. | Kinetic evaluation of PS-TTC RAFT removal using TTMSS. |
| Figure S12. | Stacked ¹ H NMR of PS-TTC and PS-H. |
| Figure S13. | SEC trace of PS-TTC. |
| Figure S14. | Kinetic evaluation of P2VP-TTC RAFT removal using EPHP. |
| Figure S15. | ¹ H NMR of P2VP-H post RAFT removal using EPHP. |
| Figure S16. | ¹ H NMR of P4VP-H post RAFT removal using EPHP. |
| Figure S17. | Kinetic comparison of RAFT end group removal using TTMSS with PMMA-TTC, P2VP-TTC, P4VP-TTC and PS-TTC |
| Figure S18. | TGA thermogram of PMMA-TTC and PMMA-H. |
| Figure S19. | TGA thermogram of P2VP-TTC and P2VP-H |
| Figure S20. | SEC trace overlay of PS-TTC and PS-H under varying concentration and solvent conditions. |
| Figure S21. | SEC trace overlay of P2VP-TTC and P2VP-H using 30:1 TTMSS to RAFT ratio and UV. |
| Figure S22. | Image of Blue light LED apparatus used for RAFT removal. |
| Figure S23. | Kinetic evaluation of P2VP-TTC RAFT removal using TTMSS and blue light. |
| Figure S24. | SEC trace overlay of P2VP-TTC and P2VP-H using UV versus blue light. |

- Figure S25. ^1H NMR integration ratios of PMMA-TTC used for end group analysis.
 Figure S26. DSC thermogram of PMMA-TTC.
 Figure S27. SEC trace of PMMA-TTC.
 Figure S28. ^1H NMR integration ratios of P2VP-TTC used for end group analysis.
 Figure S29. DSC thermogram of P2VP-TTC.
 Figure S30. SEC trace of P2VP-TTC.
 Figure S31. ^1H NMR integration ratios of P4VP-TTC used for end group analysis.
 Figure S32. DSC thermogram of P4VP-TTC.
 Figure S33. ^1H NMR integration ratios of PS-TTC used for end group analysis.
 Figure S34. DSC thermogram of PS-TTC.
 Figure S35. SEC trace of PS-TTC.
 Figure S36. ^1H NMR integration ratios of PMMA-TTC used to showing TTMSS biproduct.
 Figure S37. Absorption spectra as a function of [TTC] for PMMA-TTC
 Figure S38. Calibration curve of UV-Vis absorption as a function of [TTC] for PMMA-TTC
 Figure S39. Absorption spectra as a function of [TTC] for PS-TTC
 Figure S40. Calibration curve of UV-Vis absorption as a function of [TTC] for PS-TTC
 Figure S41. Absorption spectra as a function of [TTC] for P2VP-TTC
 Figure S42. Calibration curve of UV-Vis absorption as a function of [TTC] for P2VP-TTC
 Figure S43. Absorption spectra as a function of [TTC] for P4VP-TTC
 Figure S44. Calibration curve of UV-Vis absorption as a function of [TTC] for P4VP-TTC
 Figure S45. UV-Vis overlay of each TTC functionalized polymer showing similar λ_{max} (~310 nm) for the π to π^* transition.
 Figure S46. UV-Vis overlay for TTC functionalized polymers with zoomed inset showing n - π^* transition.
 Table S1. Tabulation of molar absorptivity and λ_{max} values for each TTC functionalized polymer.
 Figure S47. Logarithmic plot of [CTA] versus time for photoreductions using EPHP.

III. REFERENCES

p. S38

I. Experimental Procedures

Materials: All chemicals were used as received unless otherwise noted. Methyl methacrylate (MMA) (99%) and styrene (>99.9%) (inhibitor removed via passage through basic alumina prior to use), azobisisobutyronitrile (AIBN) recrystallized from methanol, 1-ethylpiperdine hypophosphite (EPHP, 95%), *N,N*-dimethylacetamide (DMAC) (>99.8%), hexanes (64% n-hexanes), 1,4-dioxane, toluene (PhMe), and methanol (MeOH) were purchased from Millipore-Sigma. 2-Vinyl pyridine (2VP, 97%) and 4-vinyl pyridine (4VP, 95%), distilled under reduced pressure before use, were purchased from Alfa-Aesar. Aluminum oxide (basic Brockman grade I) was purchased from Beantown chemical. Tris-trimethylsilylsilane (TTMSS, 97%) was obtained from Oakwood Chemical. Tetrahydrofuran (THF)

(inhibitor free) and *N,N*-dimethylformamide (DMF) were obtained from an SG Waters glass contour solvent purification system that was packed with neutral alumina and the solvents were passed through a 2 μm filter prior to being dispensed. 4-cyano-4-(dodecylsulfanylthiocarbonyl)sulfanyl pentanoic acid (CDPA) was synthesized as previously described (Figure S1).^{1,2} UV-light was emitted via 4 x 9W 365 nm bulbs (1.0 mW/cm² at 2.5 cm) installed in a readily available 36 W “MelodySusie” nail curing station. Blue light (452 nm) was generated using a WenTop® Waterproof SMD 5050 light strip containing 50 blue LEDs lining a 250 mL glass beaker (Figure S22). The measured intensity of a cluster of 5 diodes was 0.3 mW/cm² at 0.5 cm.

Characterizations: ¹H NMR experiments were conducted on a Bruker Advance III 400 MHz spectrometer in the FSU Department of Chemistry and Biochemistry NMR Laboratory. Number average molar mass (M_n) and dispersity (\mathcal{D}) of polymer samples were determined by size exclusion chromatography (SEC) on an Agilent–Wyatt combination triple detection system (THF mobile phase) containing 3 successive Agilent PLgel Mixed-C columns, an Agilent 1260 infinity series pump, degasser, autosampler, and thermostatted column chamber. The Wyatt triple detection unit hosts a mini-Dawn TREOS 3-angle light scattering detector, Optilab TrEX refractive index detector, and a Viscostar II differential viscometer. Conventional column calibration (CCC) with 10-point polystyrene (PS) standards ranging from (1800 kDa to 2 kDa) was used. Thermogravimetric analysis (TGA) was performed on a TA instruments TGA 550 by heating samples at a rate of 5 °C/min under Ar (40 mL/min flow rate) using a platinum TGA pan. Differential scanning calorimetry (DSC) analysis was performed on a TA Instruments Model Q2000 with a model RCS90 refrigerated cooling system. Samples were cycled between 25 °C and 150 °C under N₂ (40 mL/min flow rate) at a rate of 10 °C/min. Emission spectra of the blue LEDs were recorded at room temperature using an Edinburgh FLS980 fluorescence spectrometer. An intensity meter (Ophir Vega 7Z01560) with a high sensitivity power sensor (Ophir Vega 3A-FS 7Z02628) was used to measure excitation source intensities. Ultraviolet-visible (UV-vis) spectroscopy was performed on an Agilent 8453 UV-visible photodiode array spectrophotometer. Solution absorption spectra were obtained after baseline subtraction using a quartz (1 cm \times 1 cm) cuvette filled with the blank solvent. Reaction aliquots (100 μL) were taken periodically and diluted with the reaction solvent to achieve an absorbance between 2 and 2.5 O.D. at $t = 0$. The dilution of each subsequent aliquot during the reaction was kept constant. Absorbance values at 310 nm were plotted and $t_{1/2}$ values are reported as the time when the absorbance reached half its initial value at $t = 0$.

Synthesis:

Poly(methyl methacrylate) – (PMMA-TCC)

RAFT polymerization was carried out by combining MMA (8.0 g, 80 mmol), CDPA (322 mg, 0.80 mmol) and AIBN (13 mg, 0.08 mmol) [100:1:0.1, respectively] with 4.8 mL of toluene in a Schlenk flask equipped with a polytetrafluoroethylene (PTFE) stir bar. Contents were degassed by three freeze-pump-thaw cycles prior to heating at 70 °C for 7.5 h. The reaction was then cooled in an ice bath and quenched with air. Following additional dilution in THF, the polymer was collected by precipitation into a 10-fold excess of MeOH at 0 °C and filtering. The dissolution/precipitation was repeated twice more and the final collected pale yellow solids were dried at 50 °C under vacuum for 12 h. Yield (4.1 g, 51%), $M_{n,NMR} = 5.9 \text{ kg mol}^{-1}$ (determined by ^1H NMR end group analysis) (Figure S25), $M_{n,SEC} = 6.1 \text{ kg mol}^{-1}$ and $\bar{D} = 1.08$ (determined by SEC analysis) (Figure S27), $T_g = 118 \text{ °C}$ (Figure S26).

Poly(2-vinylpyridine) – (P2VP-TTC)

RAFT polymerization was carried out by combining 2VP (8.0 g, 76 mmol), CDPA (307 mg, 0.76 mmol) and AIBN (25 mg, 0.15 mmol) [100:1:0.2, respectively] with 4.5 mL of 1,4-dioxane in a Schlenk flask equipped with a PTFE stir bar. Contents were degassed by three freeze-pump-thaw cycles prior to heating at 70 °C for 15.5 h. The reaction was then cooled in an ice bath and quenched with air. Following additional dilution in THF, the polymer was collected by precipitation into a 10-fold excess of hexanes at 23 °C and filtering. The dissolution/precipitation was repeated twice more and the final collected pale orange solids were dried at 50 °C under vacuum for 12 h. Yield (6.30 g, 79%), $M_{n,NMR} = 8.3 \text{ kg mol}^{-1}$ (determined by ^1H NMR end group analysis) (Figure S28), $M_{n,SEC} = 8.5 \text{ kg mol}^{-1}$ and $\bar{D} = 1.08$ (determined by SEC analysis) (Figure S30), $T_g = 91 \text{ °C}$ (Figure S29).

Poly(4-vinylpyridine) – (P2VP-TTC)

RAFT polymerization was carried out by combining 4VP (8.0 g, 76 mmol), CDPA (304 mg, 0.75 mmol) and AIBN (25 mg, 0.15 mmol) [100:1:0.2, respectively] with 4.5 mL of DMF in a Schlenk flask equipped with a PTFE stir bar. Contents were degassed by three freeze-pump-thaw cycles prior to heating at 70 °C for 16 h. The reaction was then cooled in an ice bath and quenched with air. Following additional dilution in THF, the polymer was collected by precipitation into a 10-fold excess of hexanes at 23 °C and filtering. The dissolution/precipitation was repeated twice more and the final collected pale orange solids were dried at 50 °C under vacuum for 12 h. Yield (5.74 g, 72%), $M_{n,NMR} = 7.6 \text{ kg}$

mol⁻¹ (determined by ¹H NMR end group analysis) (Figure S31), $T_g = 137\text{ }^\circ\text{C}$ (Figure S32). P4VP was insoluble in THF and unable to be analyzed by SEC.

Polystyrene - (PS-TTC)

RAFT polymerization was carried out in bulk out by combining styrene (10.0 g, 96 mmol), CDPA (194 mg, 0.48 mmol) and AIBN (16 mg, 0.10 mmol) [100:1:0.2, respectively] in a Schlenk flask equipped with a PTFE stir bar. Contents were degassed by three freeze-pump-thaw cycles prior to heating at 80 °C for 9 h. The reaction was then cooled in an ice bath and quenched with air. Following additional dilution in toluene, the polymer was collected by precipitation into a 10-fold excess of MeOH at 23 °C and filtering. The dissolution/precipitation was repeated twice more and the final collected bright yellow solids were dried at 50 °C under vacuum for 12 h. Yield (4.01 g, 40%), $M_{n,NMR} = 7.8\text{ kg mol}^{-1}$ (determined by ¹H NMR end group analysis) (Figure S33), $M_{n,SEC} = 7.8\text{ kg mol}^{-1}$ and $\bar{D} = 1.10$ (determined by SEC analysis) (Figure S35), $T_g = 98\text{ }^\circ\text{C}$ (Figure S34).

General procedure for photoinduced removal of TTC end groups using TTMSS.

PMMA-TTC (0.30 g, 0.05 mmol TTC) and TTMSS (183 mg, 0.75 mmol) (15 mol equiv. to TTC) were dissolved in 8.9 mL THF in a 20 mL scintillation vial along with a PTFE stir bar and capped with a rubber septa. The homogenous yellow solution was sparged with Ar for 20 min before irradiating with UV light (1.0 mW/cm²) at a distance of 2.5 cm from the bulb. The temperature reached 30 ± 2 °C at this distance. For kinetic studies, aliquots were taken periodically using a syringe and ensuring the reaction solution remains under inert atmosphere. Once reaction was complete, vials were opened to atmosphere and concentrated by rotary evaporation before triplicate precipitation (MeOH) / redissolution (hexanes/THF 10:1 v/v, respectively) to remove non-polar TTMSS impurities. The collected colorless solid was dried *en vacuo* at 50 °C overnight. Left over TTMSS biproduct calculated to be approximately 2.5% of polymer mass determined using ¹H NMR integration ratios (Figure S36)

II. ADDITIONAL DATA AND FIGURES.

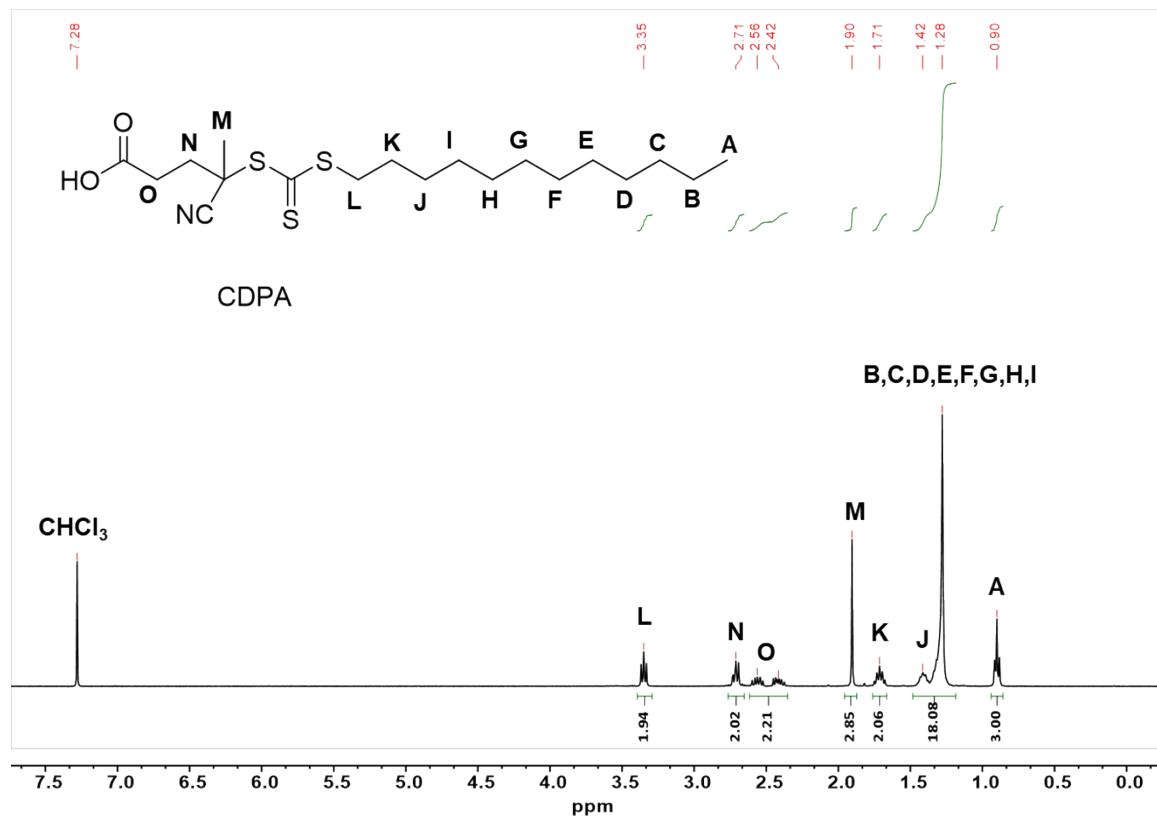


Figure S1. ¹H NMR (CDCl₃, 25 °C) of 4-cyano-4-(dodecylsulfanylthiocarbonyl)sulfanyl pentanoic acid (CDPA) RAFT CTA.

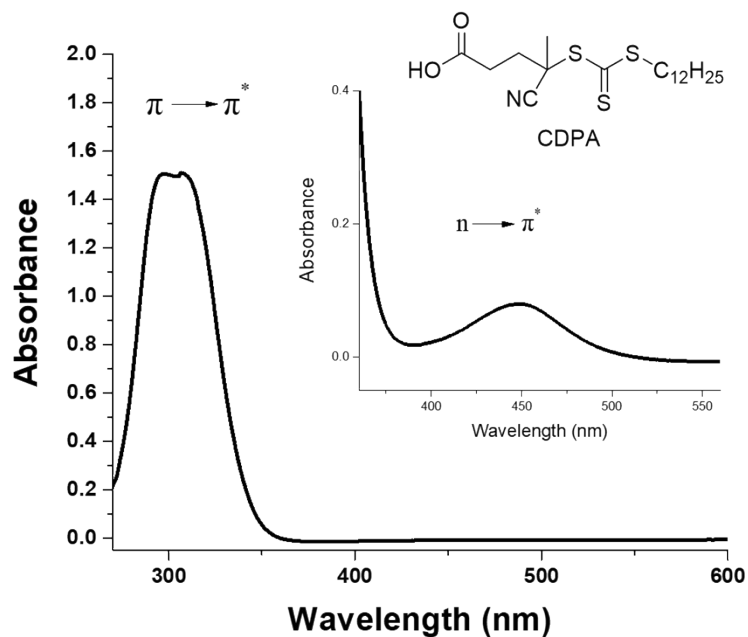


Figure S2. Absorption Spectra (CHCl₃, 23 °C) of 4-cyano-4-(dodecylsulfanylthiocarbonyl)sulfanyl pentanoic acid (CDPA) RAFT CTA.

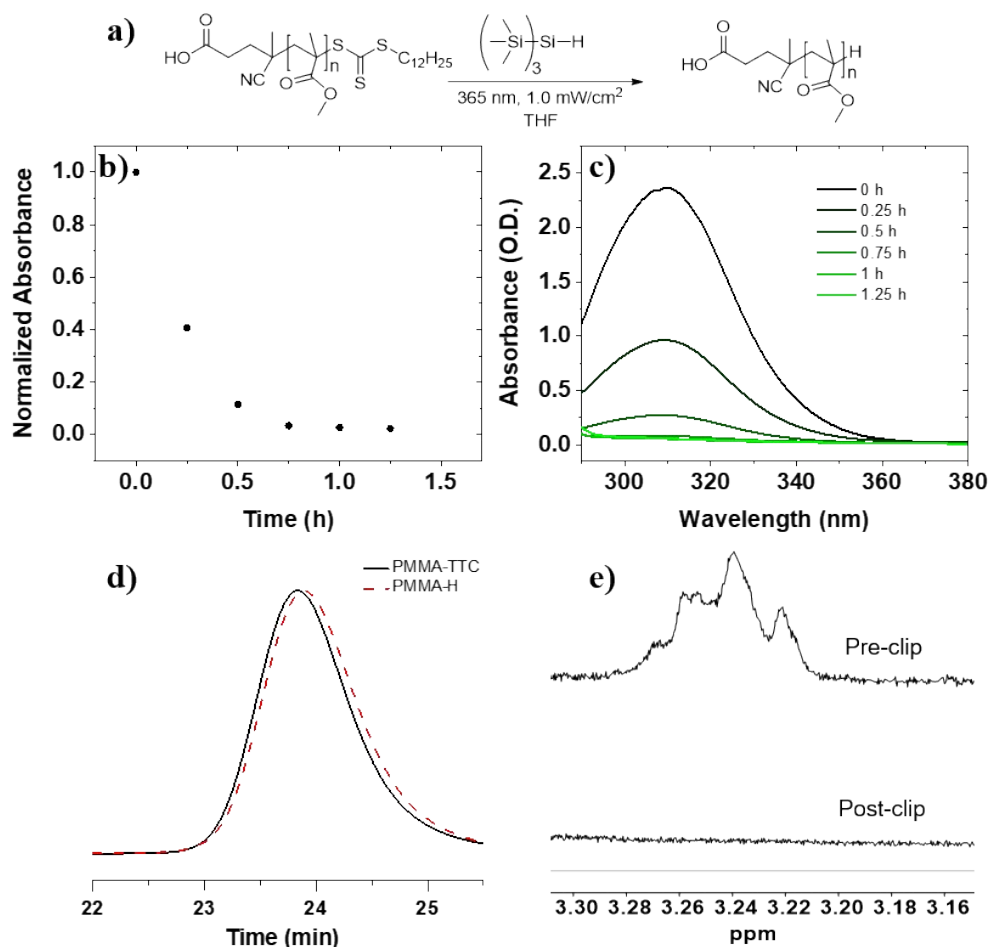


Figure S3. Removal of trithiocarbonate end group functionality from **PMMA-TTC** was complete in 1 h using a 15:1 ratio TTMSS:TTC, respectively, in THF at 5.5 mM concentration relative to TTC and 365 nm light. a) Reaction scheme for the photoinduced removal of RAFT CTA using TTMSS and UV-light. b) Normalized absorbance vs time plot for the reaction. c) UV-Vis absorption at different time intervals. d) Normalized SEC-RI trace overlay (THF mobile phase, 23 °C) before (black, solid) and after (red, dashed) the reaction. e) ^1H NMR stacked spectra of NMR region associated with the dodecyl methylene directly neighboring the TTC before (top) and after (bottom) the reaction.

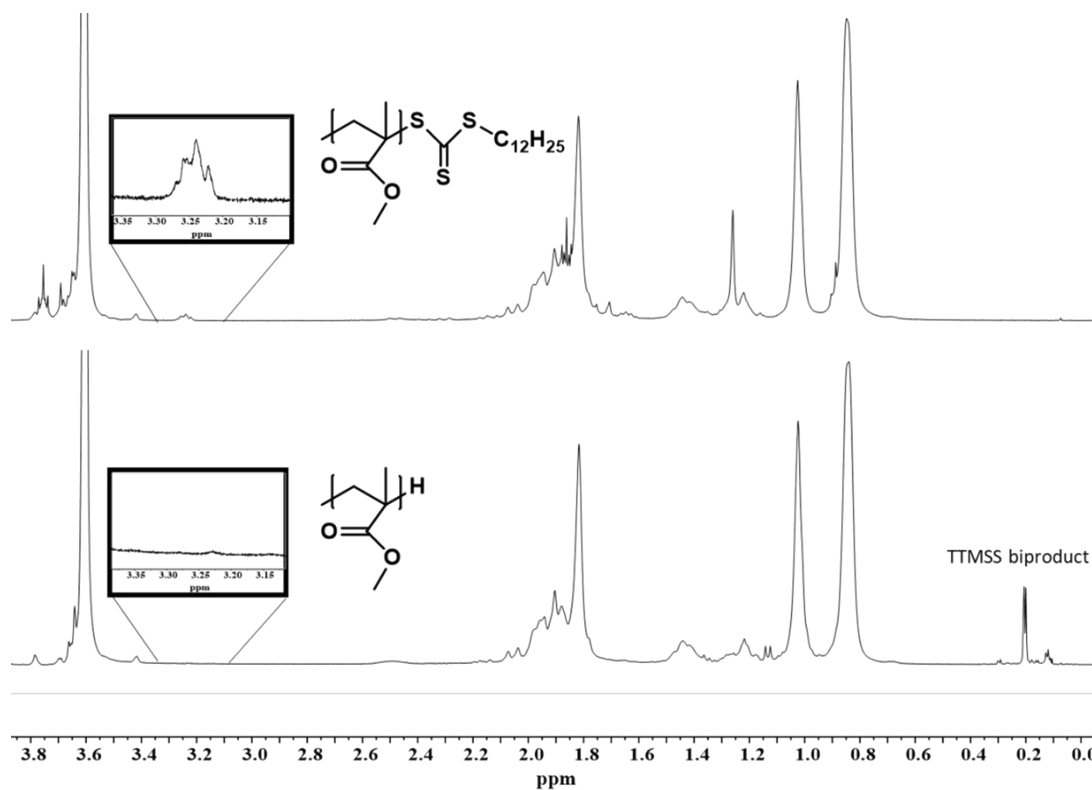


Figure S4. Stacked ¹H NMR (CDCl₃, 23 °C) of **PMMA-TTC** (top) before end group removal and **PMMA-H** (bottom) after end group removal using TTMSS.

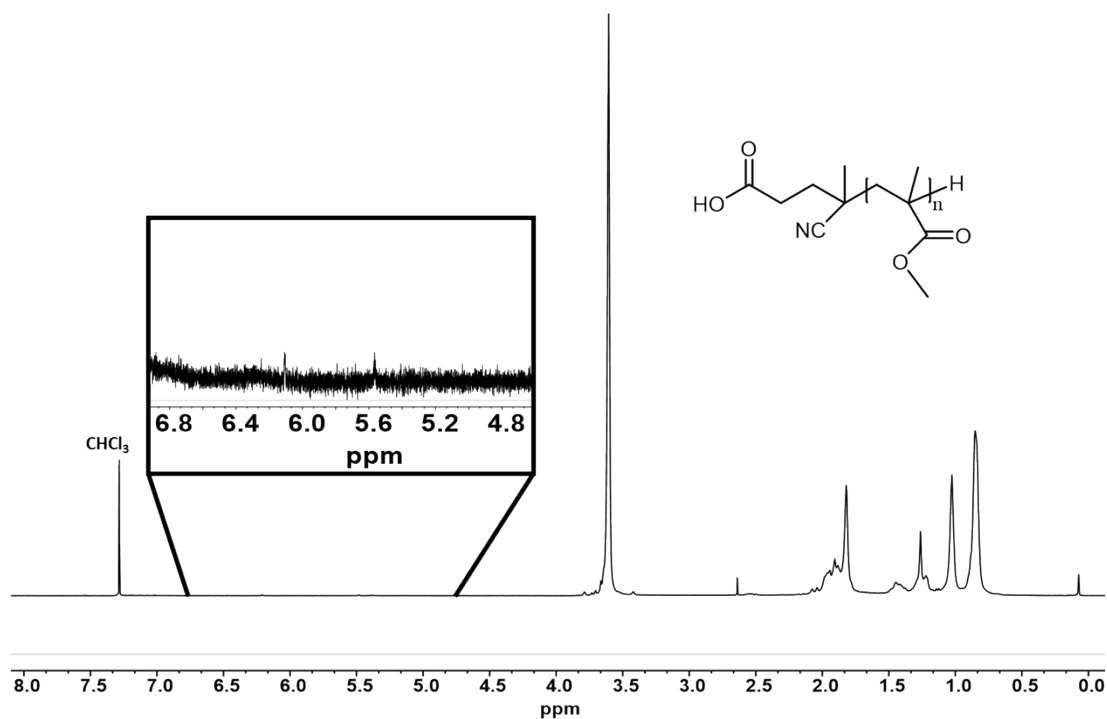


Figure S5. ¹H NMR (CDCl₃, 23 °C) of **PMMA-TTC** after end group removal using TTMSS emphasizing the olefin region to show that little to no disproportionation occurred.

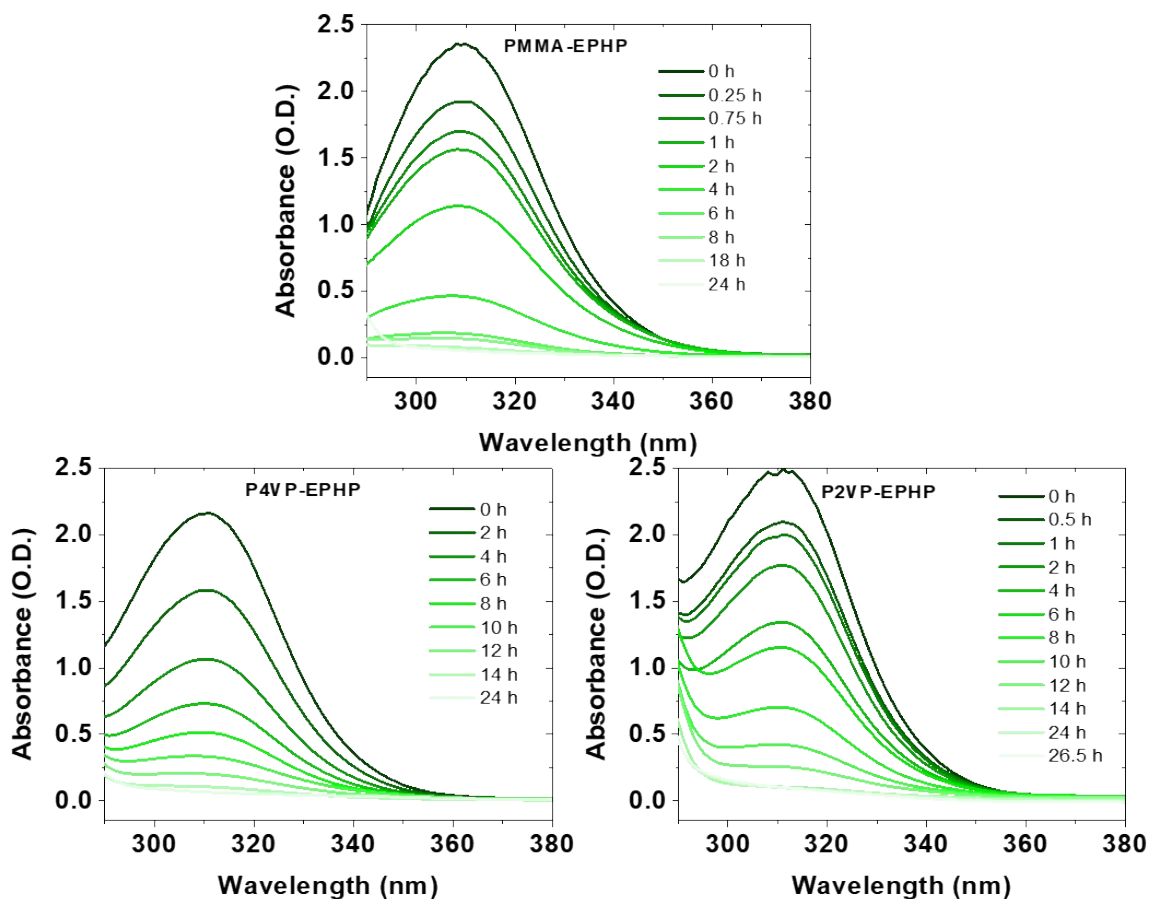


Figure S6. Absorption spectra over time for a) **PMMA-TTC**, b) **P4VP-TTC**, and c) **P2VP-TTC** under 365 nm irradiation (15:1 ratio EPHP:RAFT end respectively in THF ($[TTC]_0 = 5.5$ mM)).

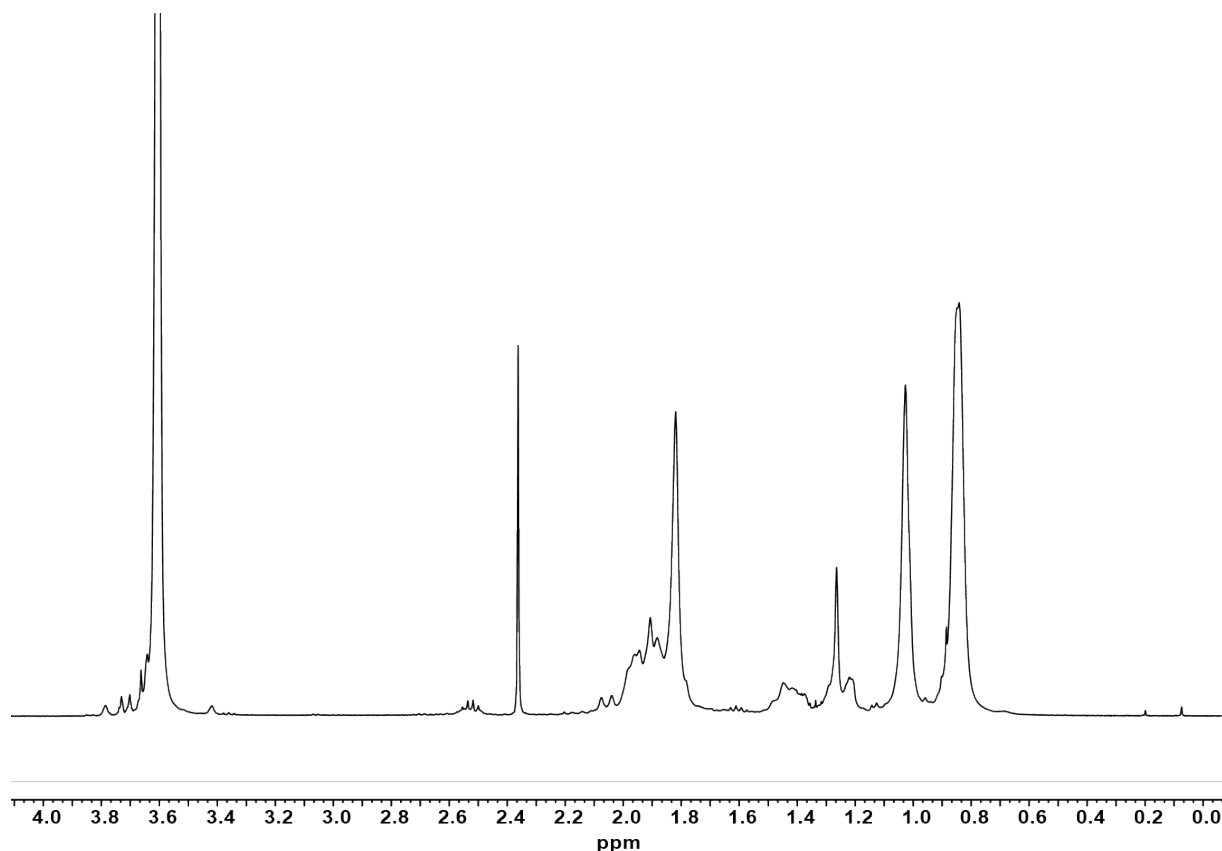


Figure S7. ^1H NMR (CDCl_3 , 23 $^\circ\text{C}$) of **PMMA-TTC** after 18 h end group removal using EPHP.

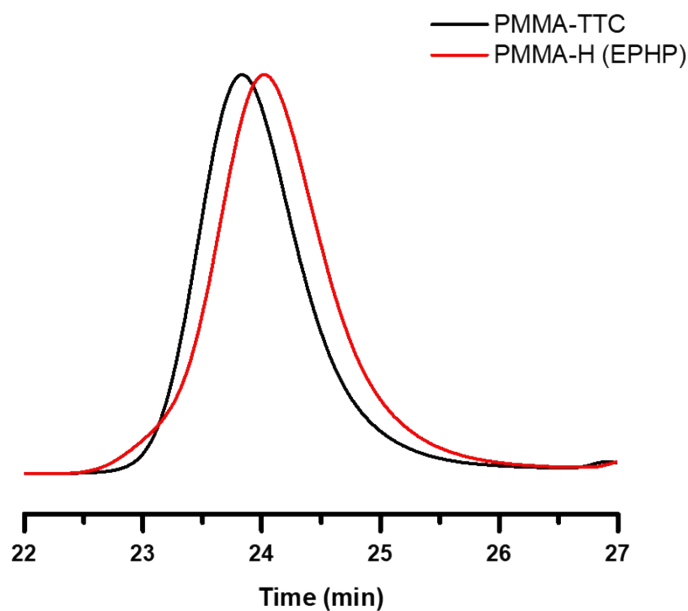


Figure S8. Normalized SEC-RI trace overlay (THF mobile phase, 23 $^\circ\text{C}$) of **PMMA-TTC** (black) before photoinduced RAFT removal and **PMMA-H** (red) post-removal RAFT removal using 15:1 ratio EPHP:RAFT end respectively in THF with $[\text{TTC}]_0 = 5.5 \text{ mM}$ and 365 nm UV light.

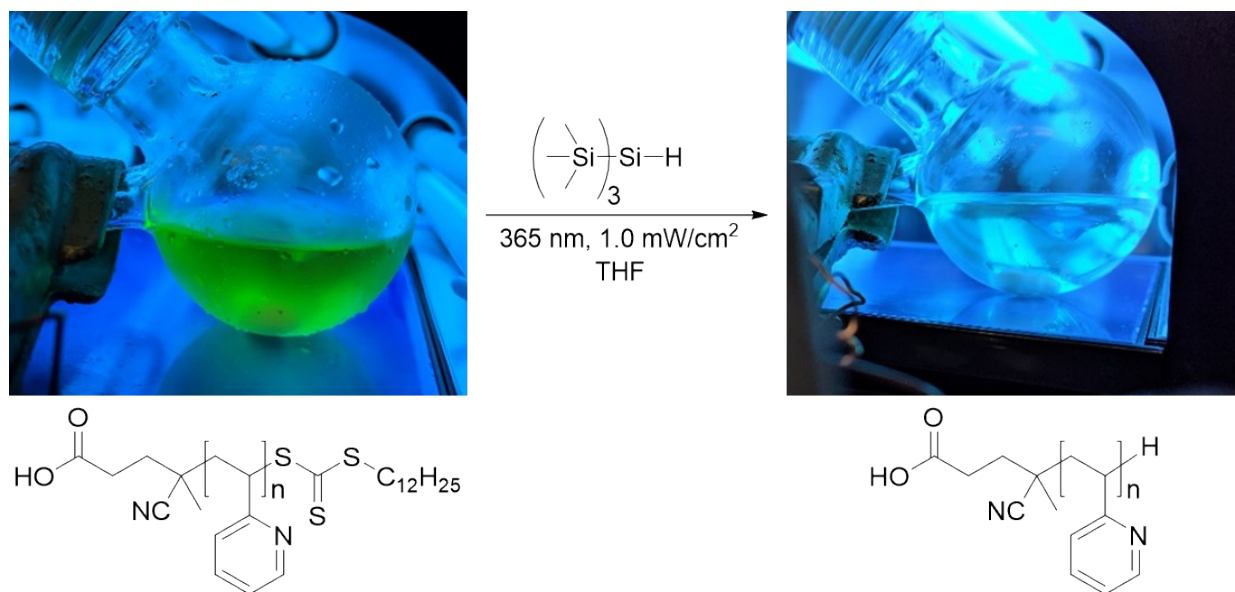


Figure S9. Photographs of P2VP-TTC before (left) and after (right) 365 nm irradiation.

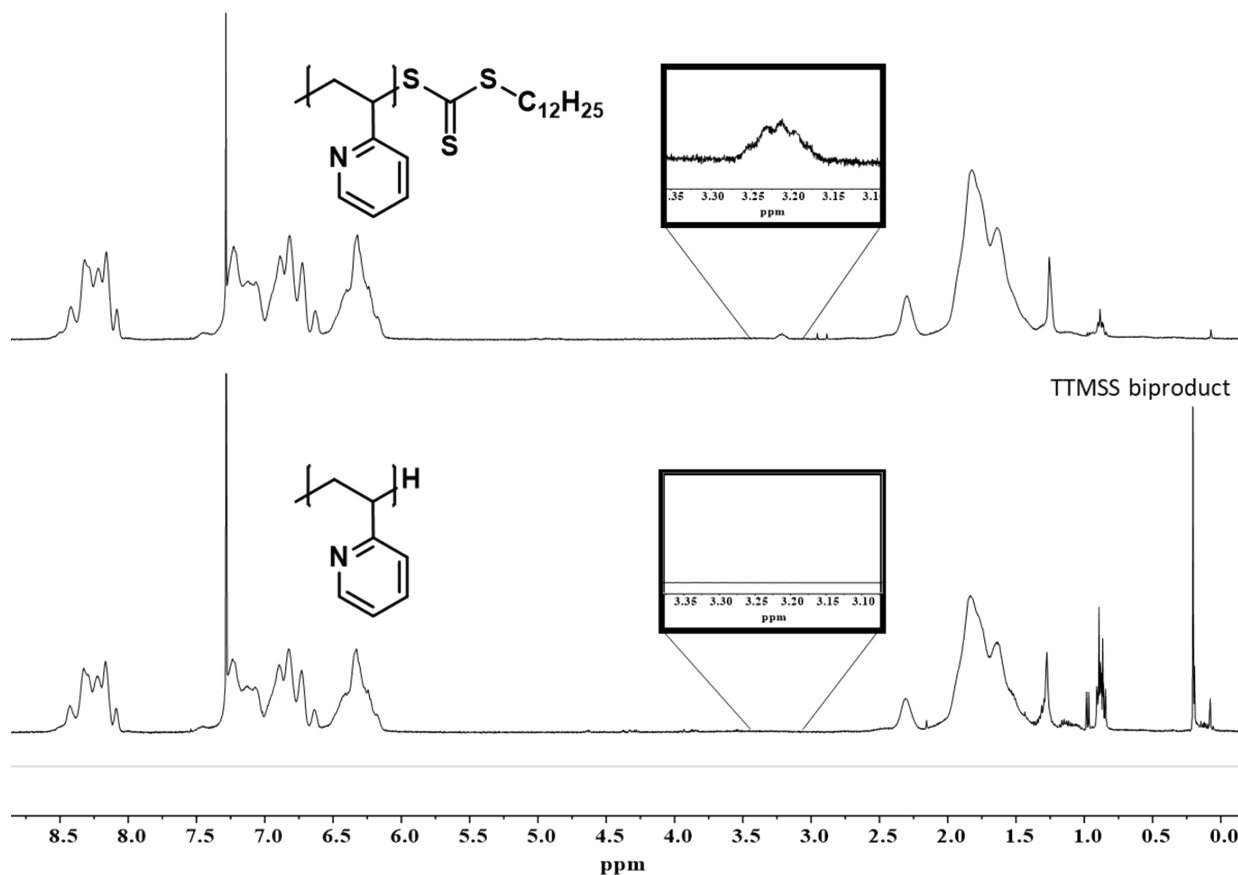


Figure S10. Stacked ^1H NMR (CDCl_3 , 23 $^\circ\text{C}$) of **P2VP-TTC** (top) before end group removal and **P2VP-H** (bottom) after end group removal using TTMSS.

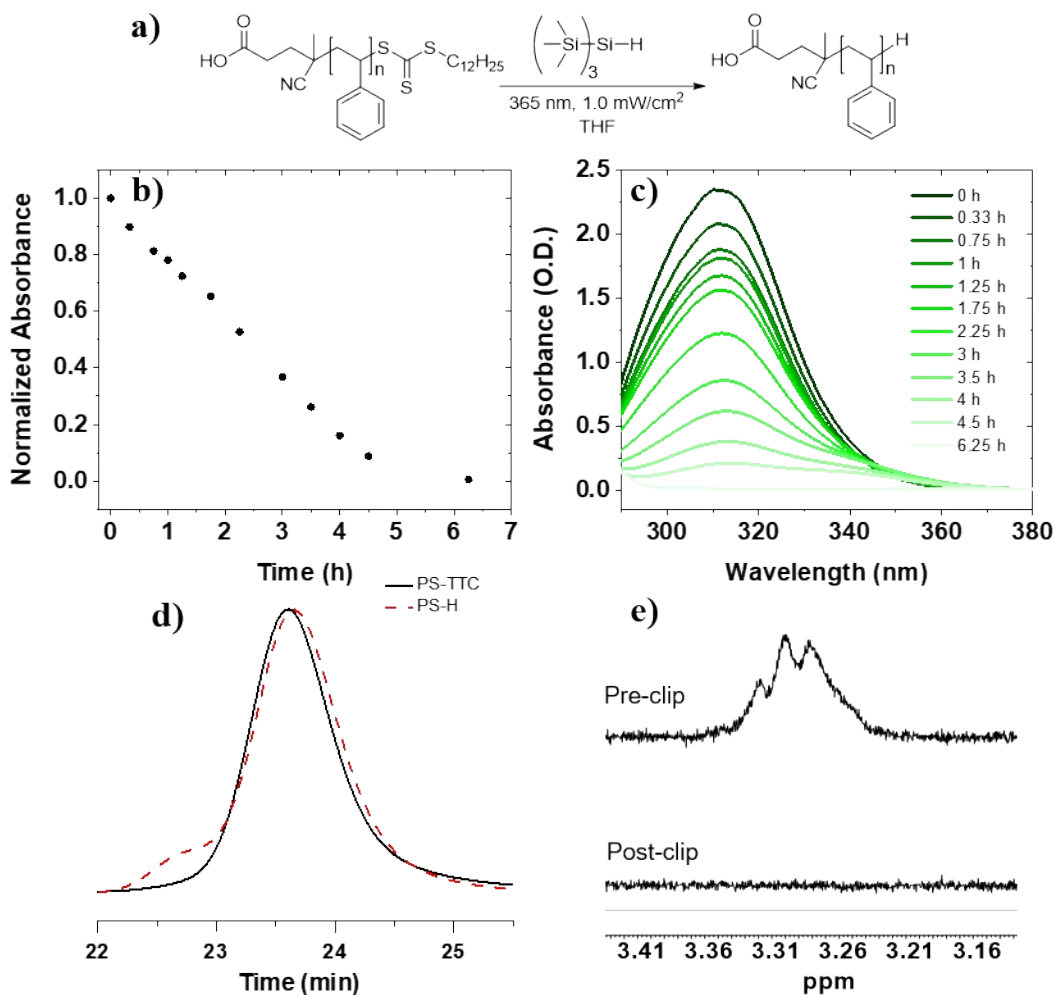


Figure S11. a) Reaction scheme for photoinduced ($\lambda = 365$ nm) removal of TTC from **PS-TTC** in THF ($[\text{TTC}]_0 = 5.5$ mM) using TTMSS:TTC of 15:1. b) Normalized absorbance at 309 nm as a function of irradiation time. c) UV-Vis absorption spectra from aliquots taken at known time intervals throughout the reaction. d) Normalized SEC-RI trace overlay (THF mobile phase, 23 °C) of **PS-TTC** before (black solid) and after (red dashed) the reaction. e) Offset ^1H NMR (CDCl_3 , 25 °C) spectra of methylene proton signal ($\text{S-CH}_2\text{-C}_{11}\text{H}_{23}$) before (top) and after (bottom) the reaction.

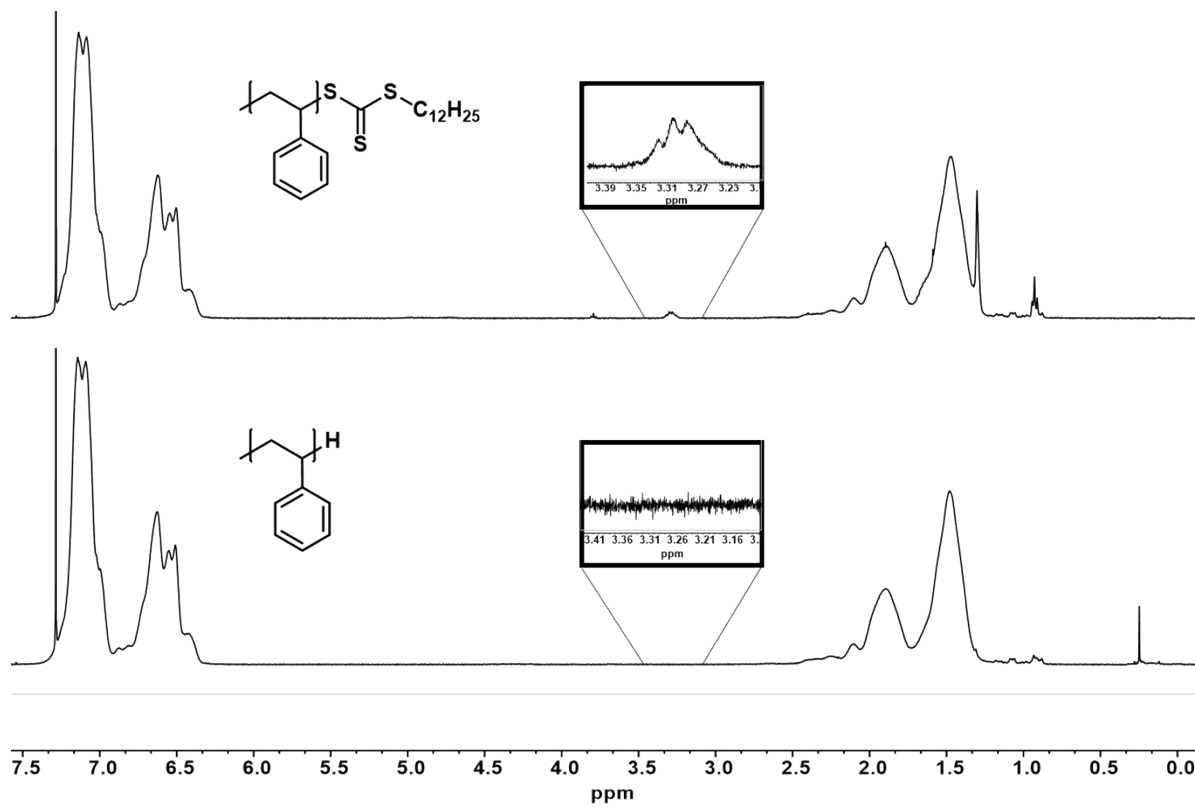


Figure S12. Stacked ^1H NMR (CDCl_3 , 23 $^\circ\text{C}$) of PS-TTC (top) before and (bottom) after reduction using TTMSS.

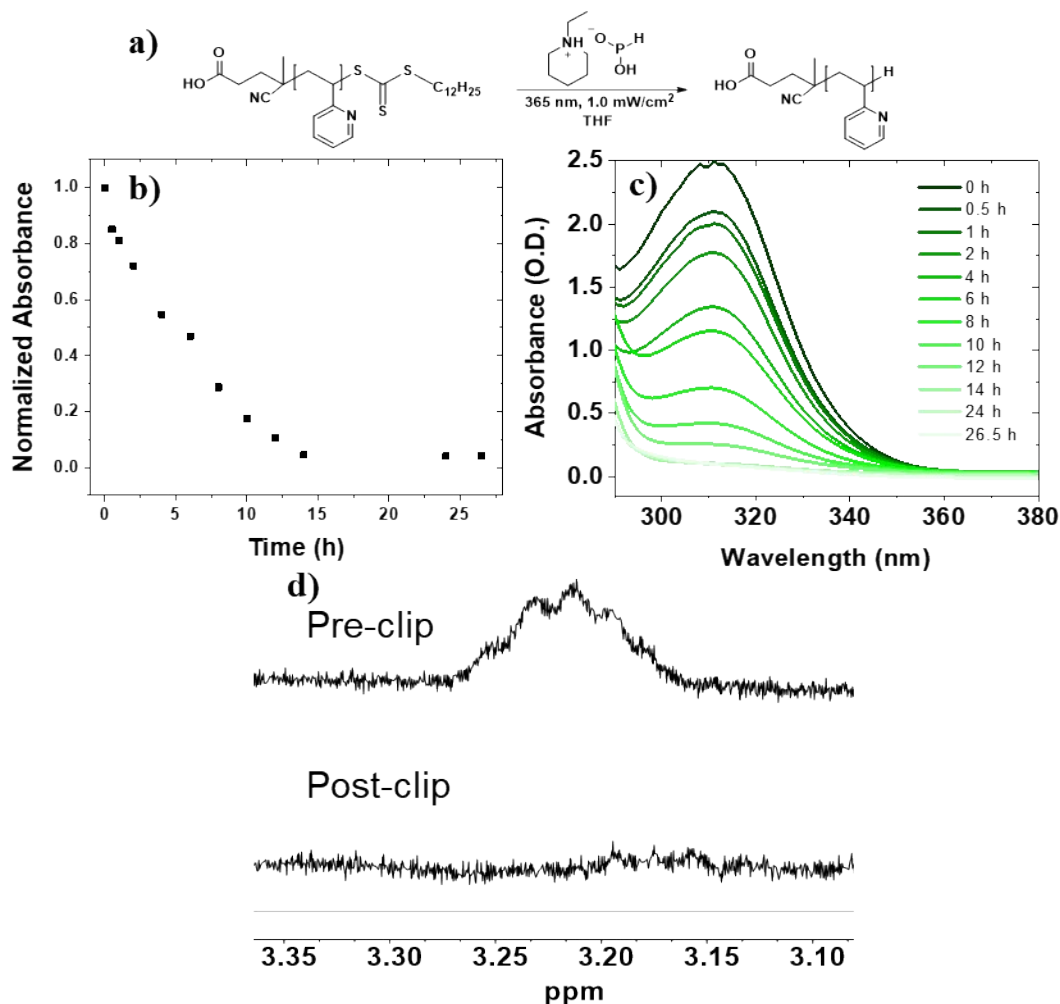


Figure S13. Removal of trithiocarbonate end group functionality from **P2VP-TTC** was complete in 26.5 h using a 15:1 ratio EPHP:RAFT end respectively in THF ($[TTC]_0 = 5.5$ mM) and 365 nm UV light. a) Reaction scheme for the photoinduced removal of RAFT CTA using EPHP and UV-light. b) Normalized absorbance vs time plot for the reaction. c) UV-Vis absorption spectra at different time intervals. Final ABS was found to be 0.12 after 26.5 h d) Offset ^1H NMR stacked spectra of NMR region associated with the dodecyl methylene directly neighboring the trithiocarbonate of **P2VP-TTC** before (top) and after (bottom) the reaction.

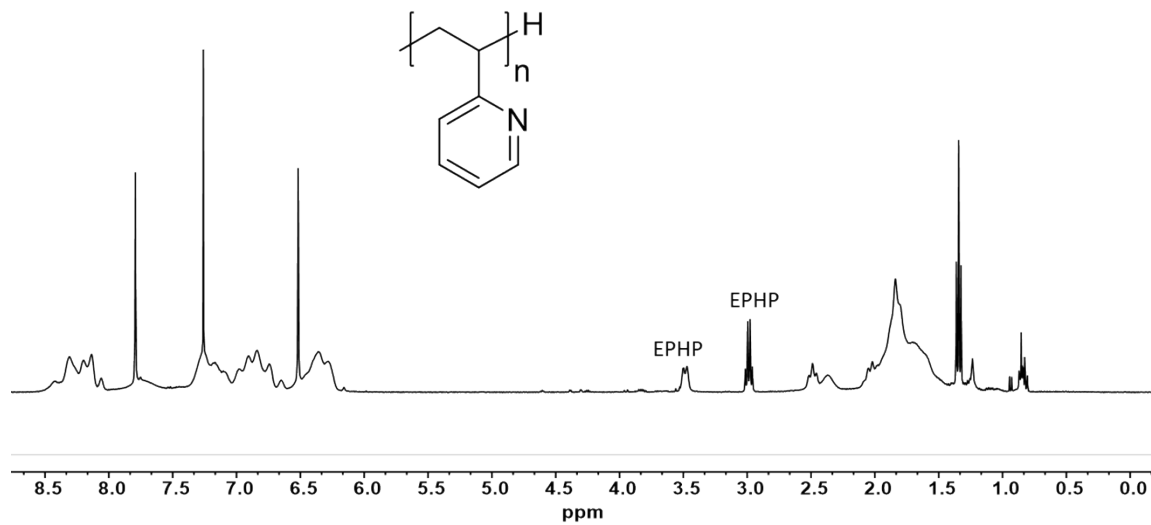


Figure S14. $^1\text{H NMR}$ (CDCl₃, 23 °C) of **P2VP-TTC** after 26.5 h end group removal using EPHP.

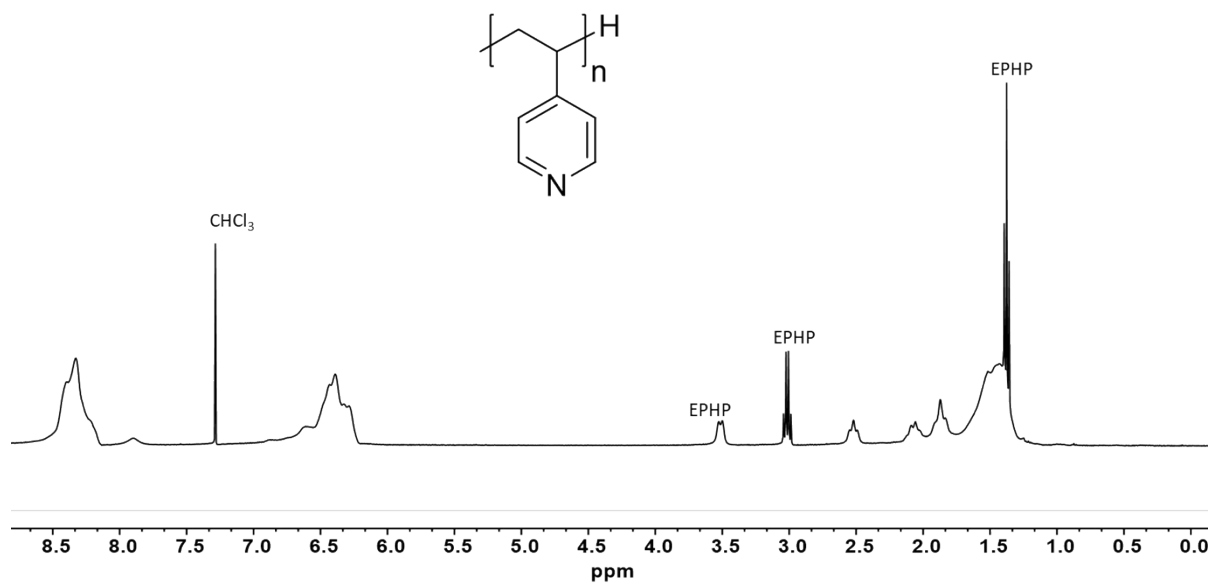


Figure S15. $^1\text{H NMR}$ (CDCl₃, 600 MHz, 23 °C) of **P4VP-H** after 24 h end group removal using EPHP.

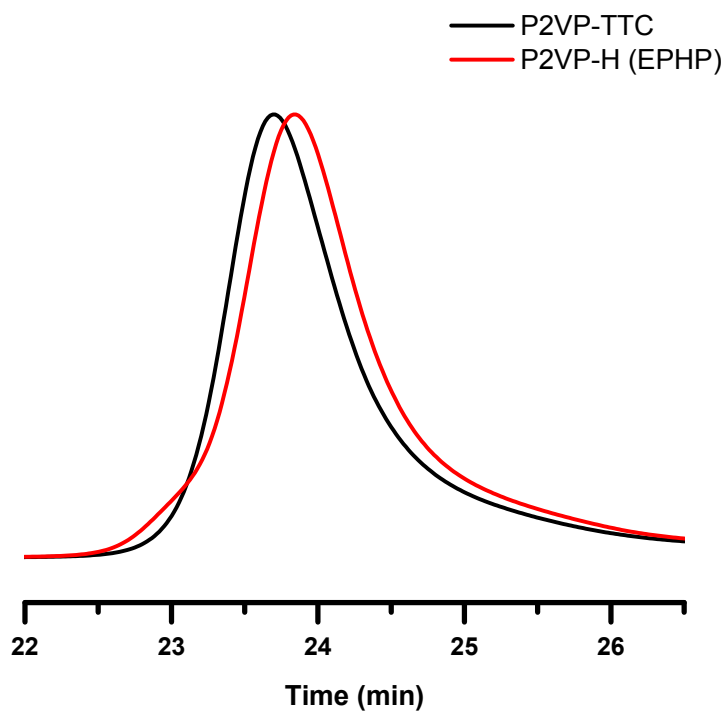


Figure S16. Normalized SEC-RI trace overlay (THF mobile phase, 23 °C) of **P2VP-TTC** (black) before photoinduced RAFT removal and **P2VP-H** (red) post-removal RAFT removal using 15:1 ratio EPHP:RAFT end respectively in THF with $[TTC]_0 = 5.5$ mM and 365 nm light.

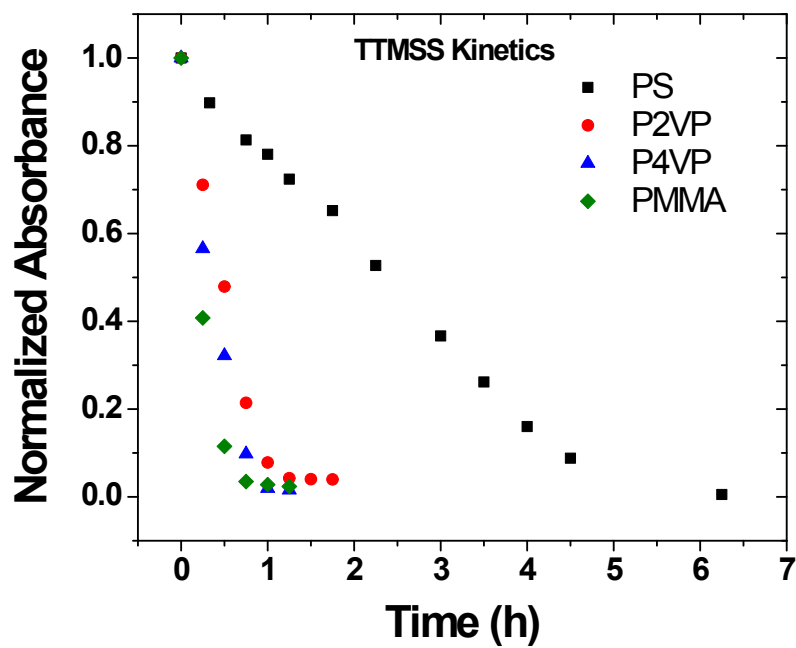


Figure S17. Normalized absorbance vs time plot for the 365 nm irradiation of **PMMA-TTC**, **P2VP-TTC**, and **P4VP-TTC** reaction mixtures (15:1 TTMSS:RAFT ($[TTC]_0 = 5.5$ mM) in THF).

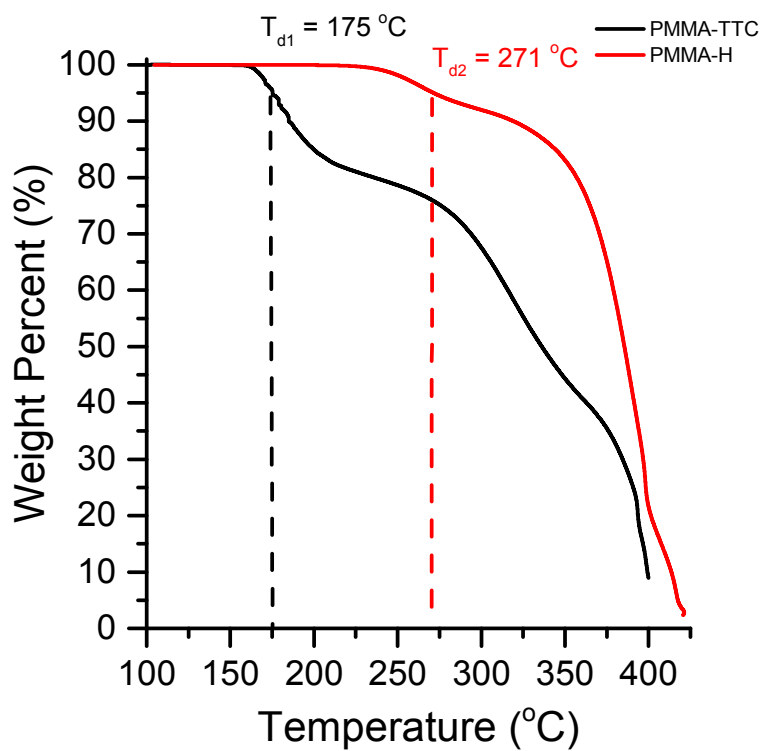


Figure S18. TGA thermogram overlay of **PMMA-TTC** before RAFT removal and **PMMA-H** after RAFT removal using TTMS taken at a heating rate of 5 °C min^{-1} under Ar flow. The thermal decomposition temperature (T_{d1} and T_{d2}) are defined at the point where 5% mass loss has occurred.

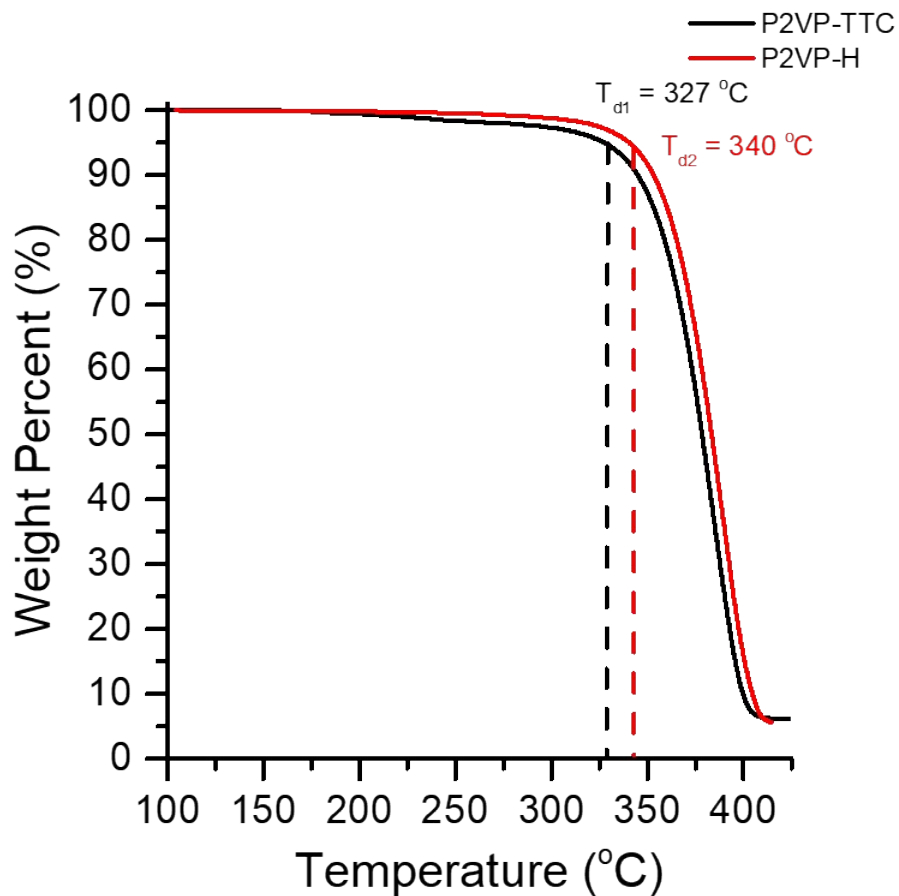


Figure S19. TGA thermogram overlay of **P2VP-TTC** and **P2VP-H** after reduction with TTMSS using a heating rate of $5\text{ }^{\circ}\text{C min}^{-1}$ under Ar. The thermal decomposition temperatures (T_{d1} and T_{d2}) are defined at the point where 5% mass loss has occurred.

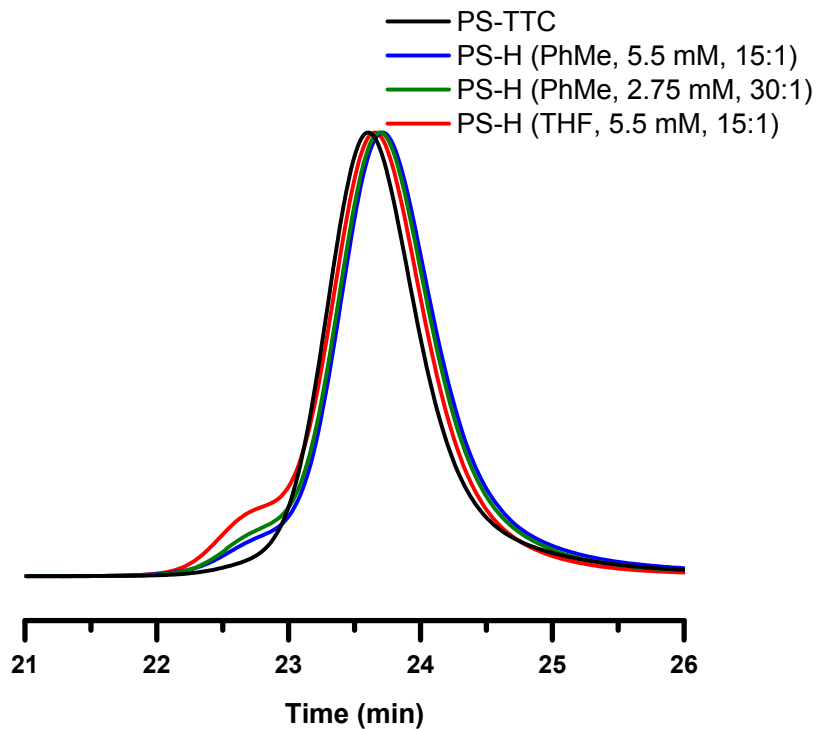


Figure S20. Normalized SEC-RI trace overlay (THF mobile phase, 23 °C) of **PS-TTC** (black) before photoinduced RAFT removal, **PS-H** (blue) post-removal RAFT removal using 15:1 ratio TTMSS:RAFT end respectively in toluene at 5.5 mM, **PS-H** (green) post-removal RAFT removal using 30:1 ratio TTMSS:RAFT end respectively in THF at 2.75 mM, **PS-H**, (red) post-removal RAFT removal using 15:1 ratio TTMSS:RAFT end respectively in THF at 5.5 mM. Concentrations are relative to the RAFT CTA chain end and performed under 365 nm light.

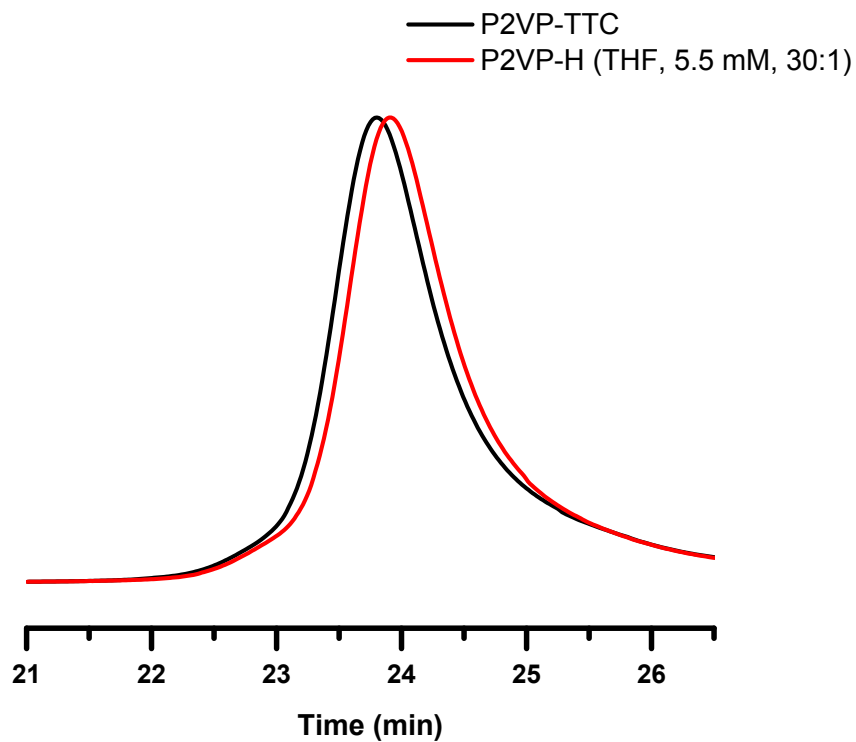


Figure S21. Normalized SEC-RI trace overlay (THF mobile phase, 23 °C) of **P2VP-TTC** (black) before photoinduced RAFT removal and **P2VP-H** (red) post-removal RAFT removal using 30:1 ratio TTMSS:RAFT end respectively in THF ($[TTC]_0 = 5.5 \text{ mM}$) and 365 nm light.



Figure S22. Photograph of the apparatus used for RAFT removal using a 50 LED strip (452 nm). Intensity was measured as 0.3 mW/cm² from 5 clustered LEDs at a distance of 0.5 cm.

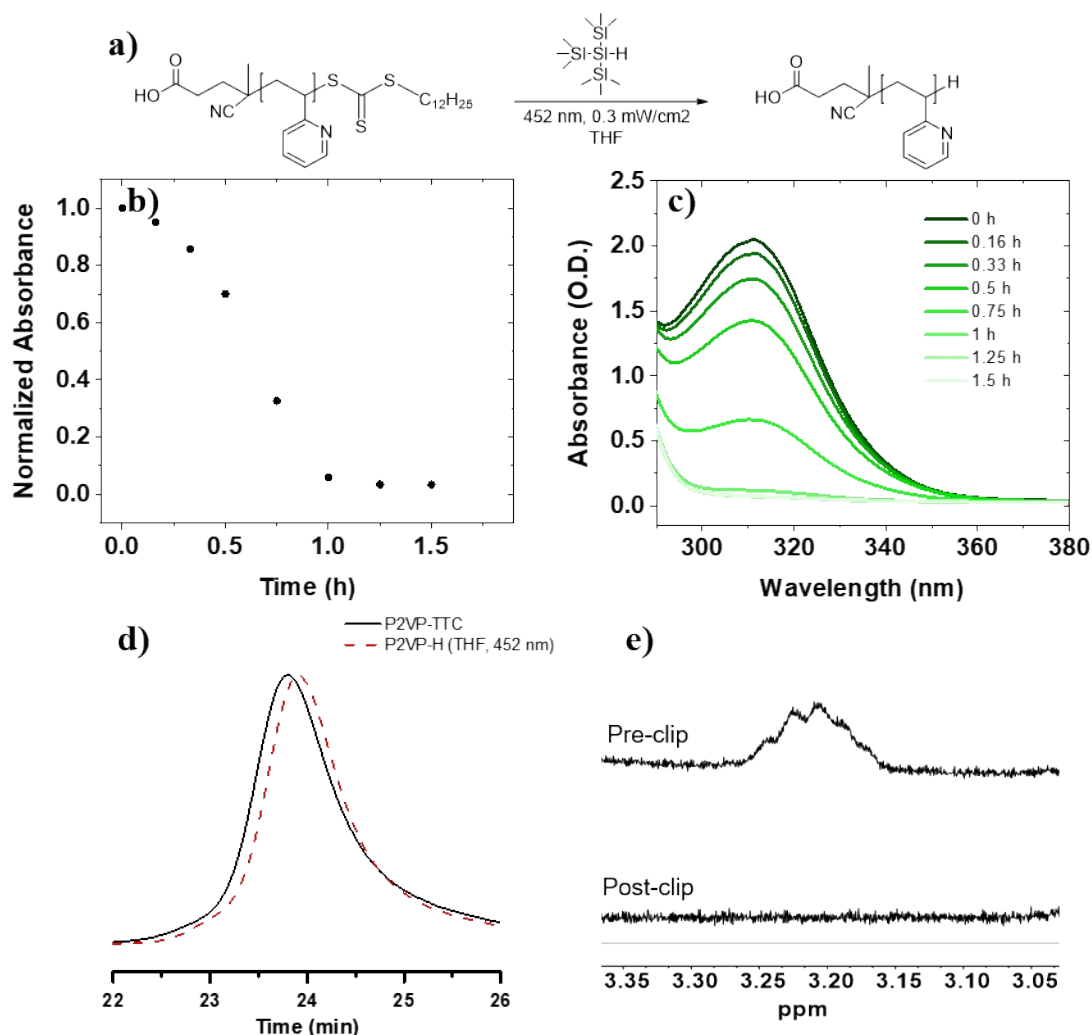


Figure S23. Removal of trithiocarbonate end group functionality from **P2VP-TTC** was complete in 1.25 h using a 15:1 ratio TTMSS:RAFT end respectively in THF ($[TTC]_0 = 5.5$ mM) and 452 nm blue light. . a) Reaction scheme for the photoinduced removal of RAFT CTA using TTMSS and blue light. b) Normalized absorbance vs time plot for the reaction. c) UV-Vis absorption spectra at different time intervals during the reaction. d) Normalized SEC-RI trace overlay (THF mobile phase, 23 °C) of **P2VP-TTC** before (black) and after (red) the reaction. e) Offset ^1H NMR spectra of NMR region associated with the dodecyl methylene directly neighboring the trithiocarbonate of **P2VP-TTC** before (top) and after (bottom) the reaction.

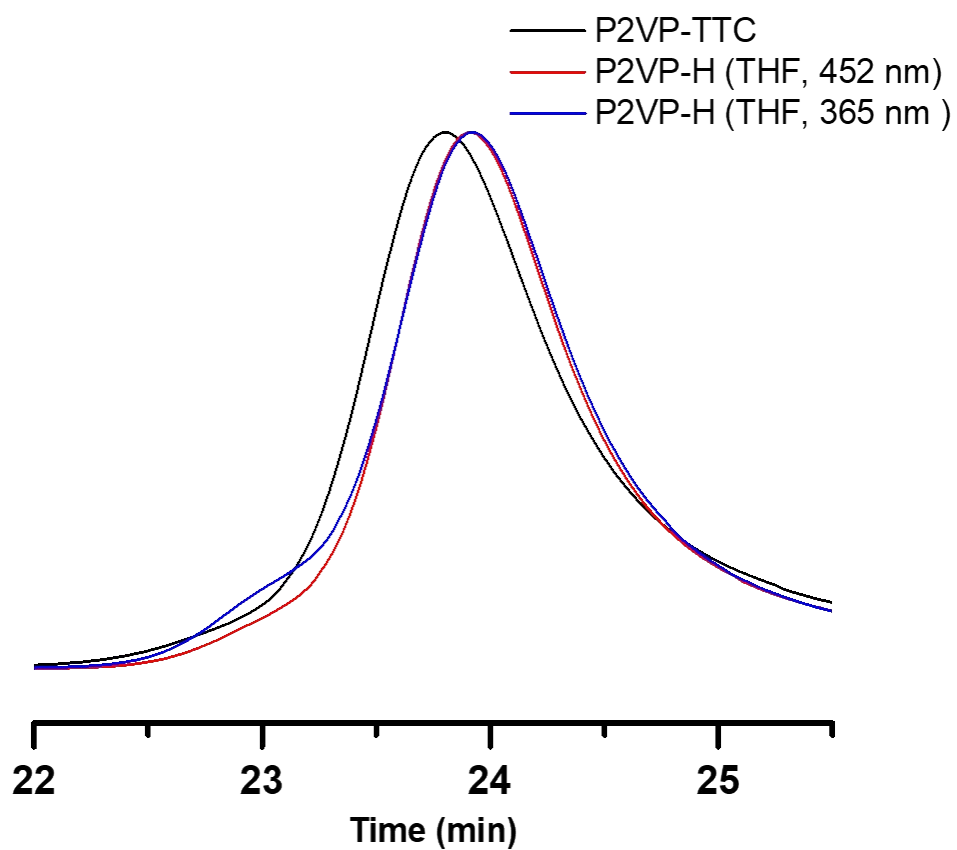


Figure S24. Normalized SEC-RI trace overlay (THF mobile phase, 23 °C) of **P2VP-TTC** (black) before photoinduced RAFT removal, **P2VP-H** (red) post-removal RAFT removal using 452 nm light, and **P2VP-H** (blue) post-removal RAFT removal using 365 nm light. Both reactions performed with a 15:1 ratio TTMSS:RAFT end respectively in THF at 5.5 mM concentration relative to RAFT CTA.

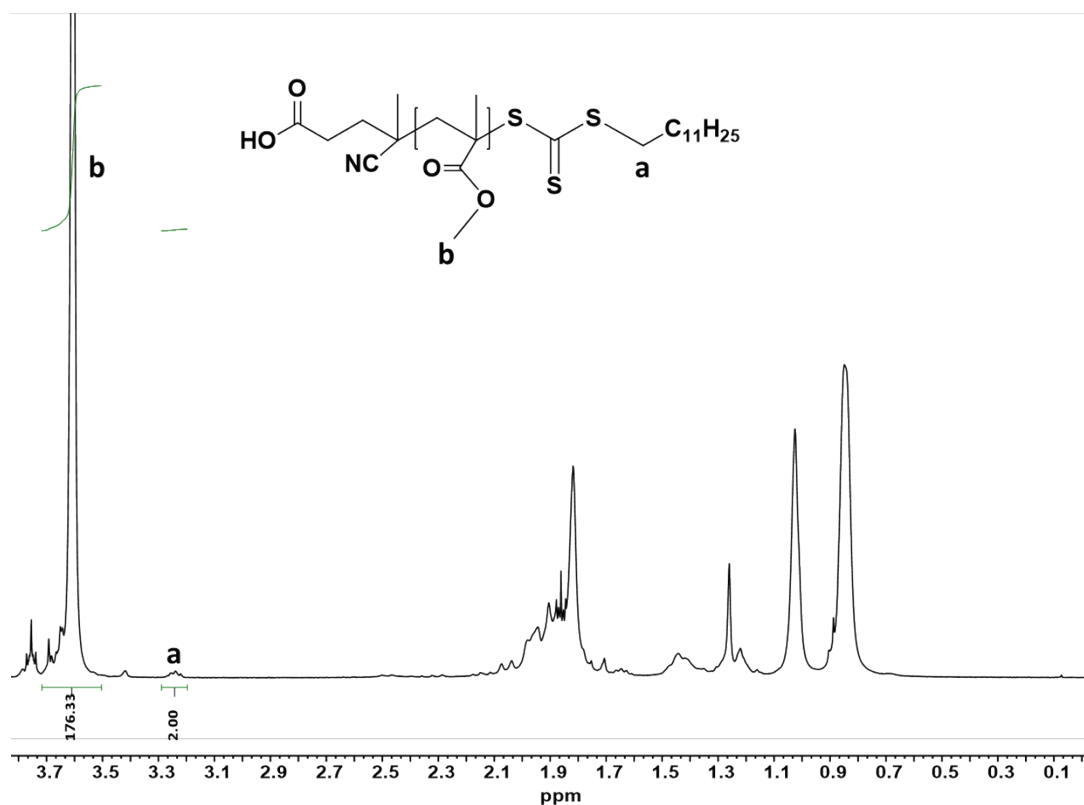


Figure S25. ^1H NMR (CDCl_3 , 23 $^\circ\text{C}$) of **PMMA-TTC** spectra showing the integration ratios used for determining molecular weight via end group analysis.

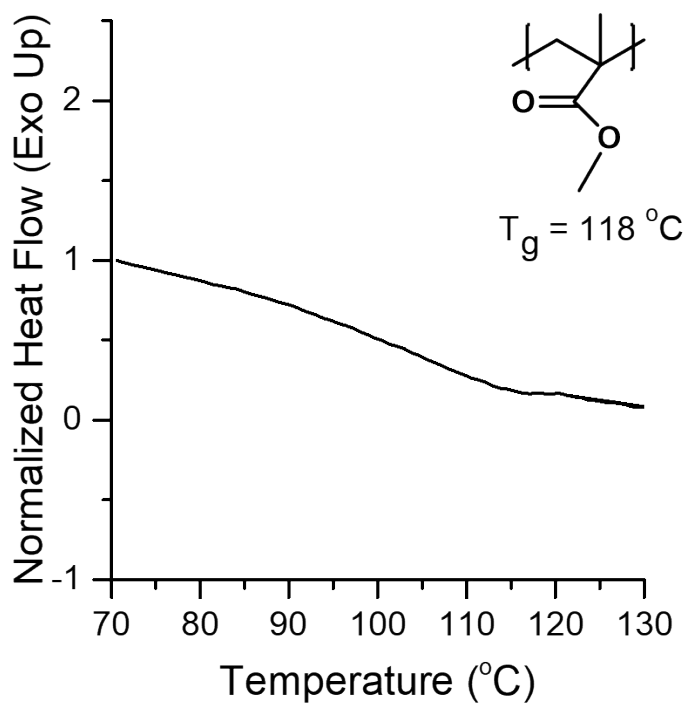


Figure S26. DSC thermogram of **PMMA-TTC** (exo up) before RAFT clipping. Samples were cycled from 25 $^\circ\text{C}$ to 150 $^\circ\text{C}$ at a rate of 10 $^\circ\text{C min}^{-1}$ under N_2 . Data displayed is the 2nd heating.

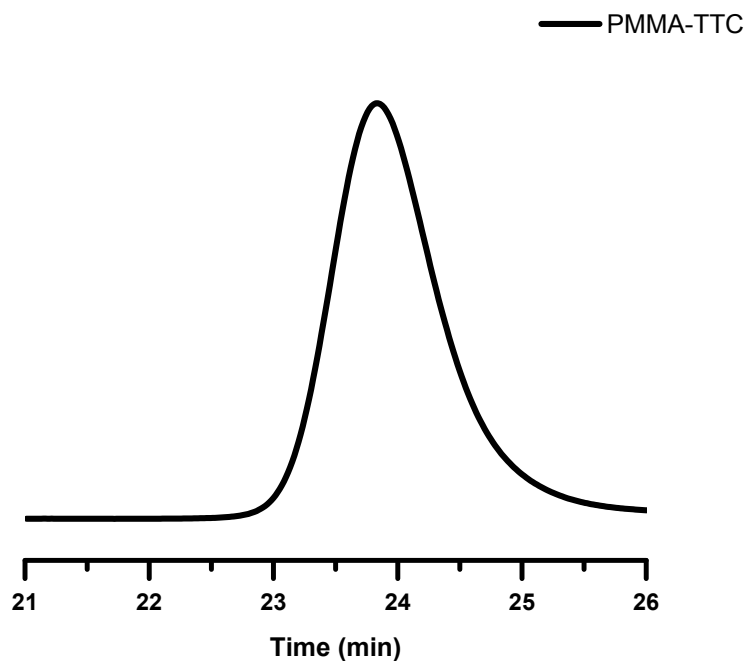


Figure S27. Normalized SEC-RI trace (THF mobile phase, 25 °C) of **PMMA-TTC** poly(methyl methacrylate) homopolymer before photoinduced RAFT clipping ($M_n = 7.8$ kDa, $\bar{D} = 1.08$) determined by conventional column calibration using PS standards.

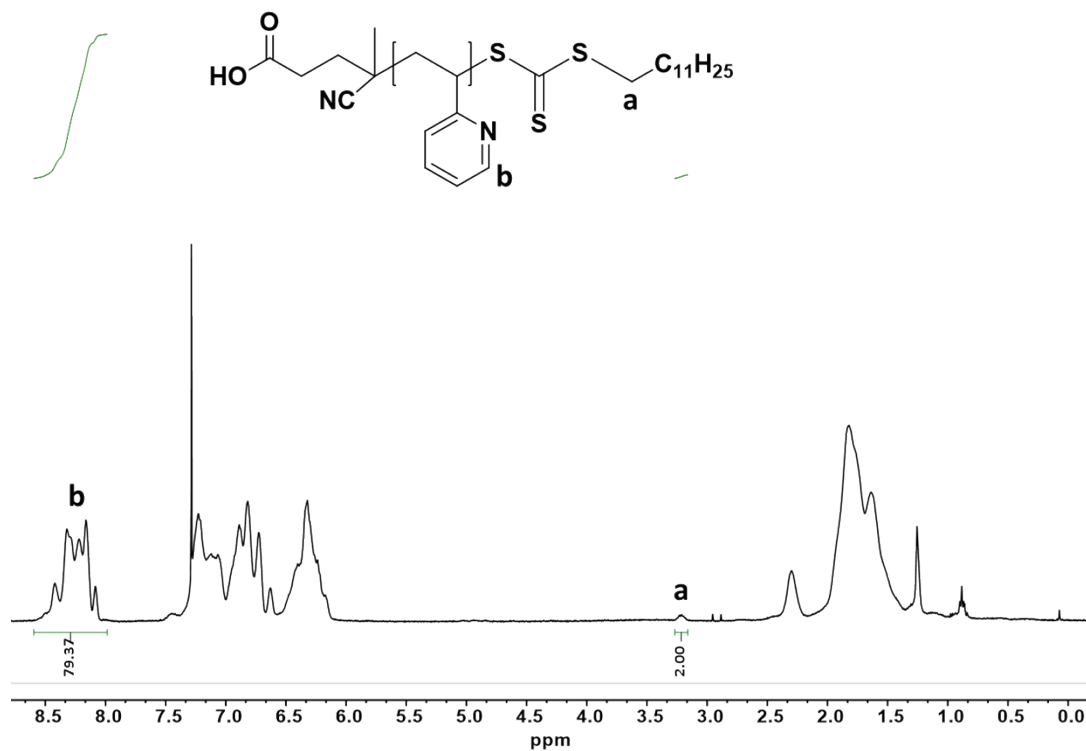


Figure S28. $^1\text{H NMR}$ (CDCl₃, 23 °C) of **P2VP-TTC** spectra showing the integration ratios used for determining molecular weight via end group analysis.

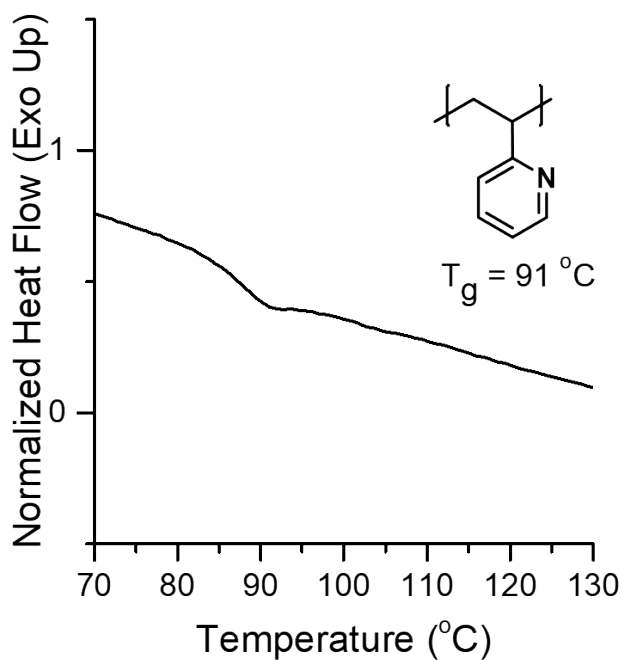


Figure S29. DSC thermogram of **P2VP-TTC** (exo up) before RAFT clipping. Samples were cycled from 25 °C to 150 °C at a rate of 10 °C min⁻¹ under N₂. Data displayed is the 2nd heating.

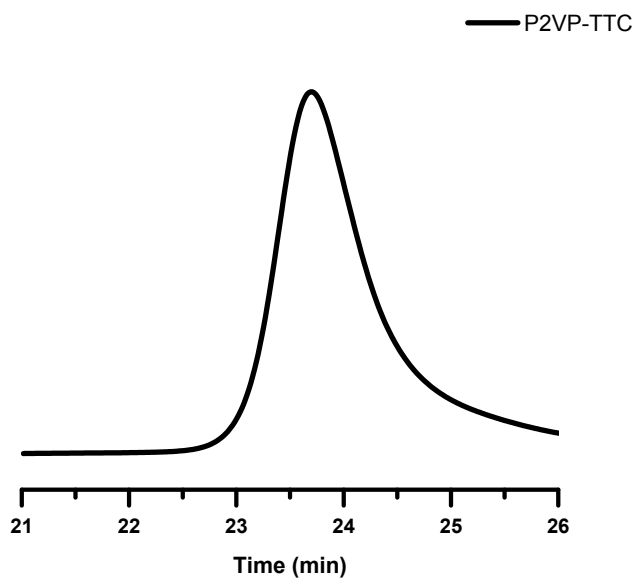


Figure S30. Normalized SEC-RI trace (THF mobile phase, 25 °C) of **P2VP-TTC** poly(2-vinylpyridine) homopolymer before photoinduced RAFT clipping ($M_n = 8.3\text{ kDa}$, $\mathcal{D} = 1.09$) and determined by conventional column calibration using PS standards.

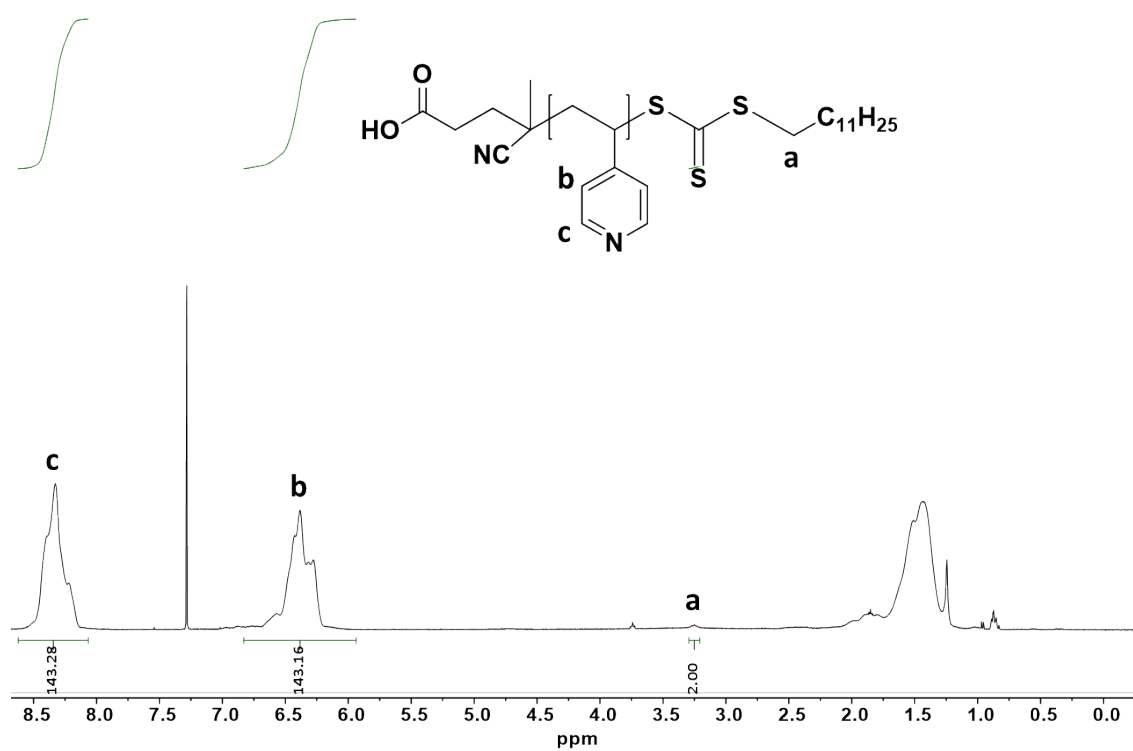


Figure S31. ¹H NMR (CDCl₃, 23 °C) of P4VP-TTC spectra showing the integration ratios used for determining molecular weight via end group analysis.

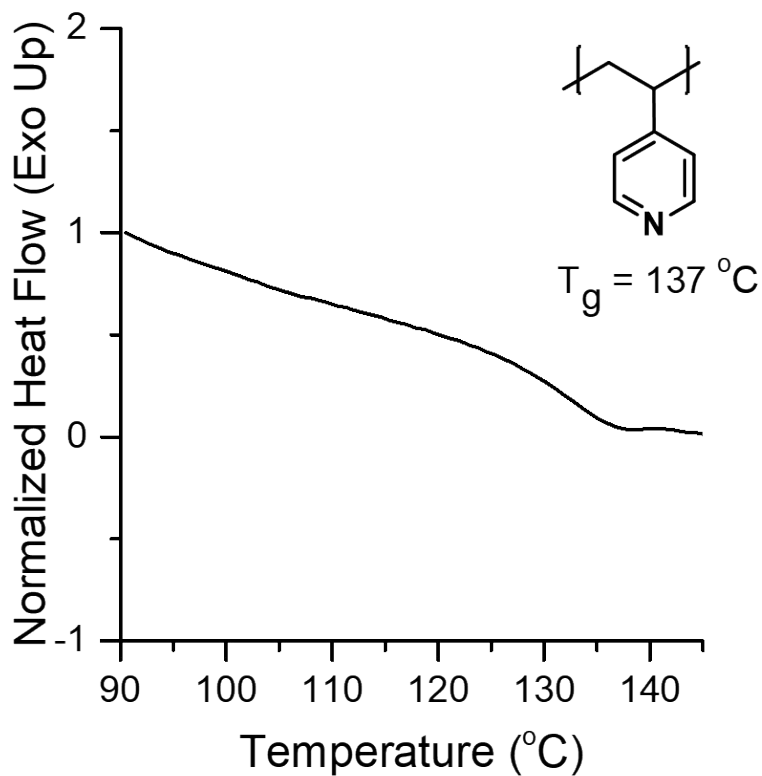


Figure S32. DSC thermogram of P4VP-TTC (exo up) before RAFT clipping. Samples were cycled from 25 °C to 150°C at a rate of 10 °C min⁻¹ under N₂. Data displayed is the 2nd heating.

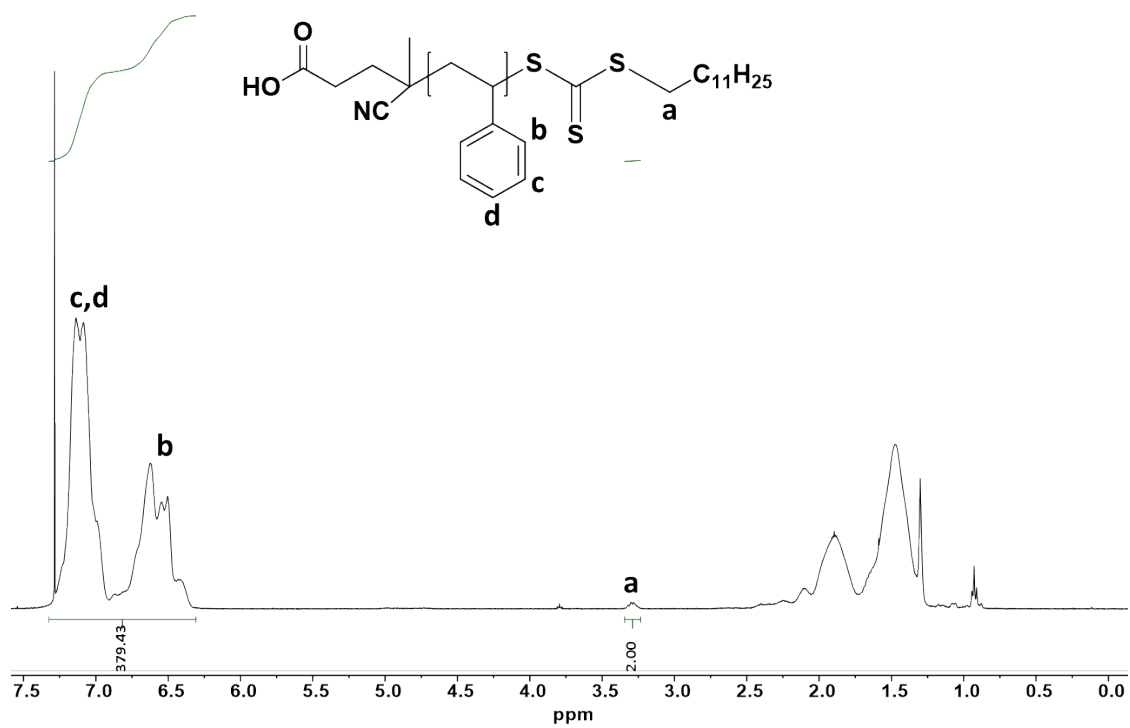


Figure S33. ¹H NMR (CDCl₃, 23 °C) of PS-TTC spectra showing the integration ratios used for determining molecular weight via end group analysis.

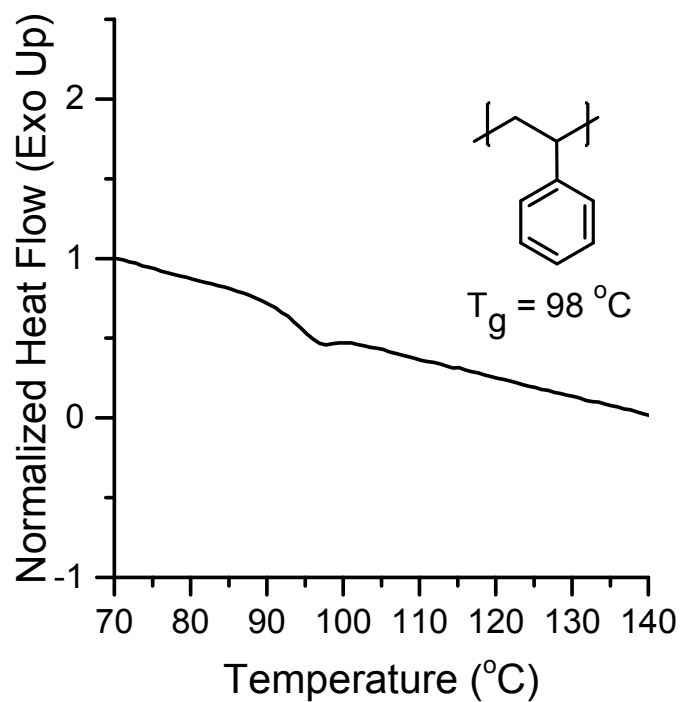


Figure S34. DSC thermogram of **PS-TTC** (exo up) before RAFT clipping. Samples were cycled from 25 °C to 150 °C at a rate of 10 °C min⁻¹ under N₂. Data displayed is the 3rd heating.

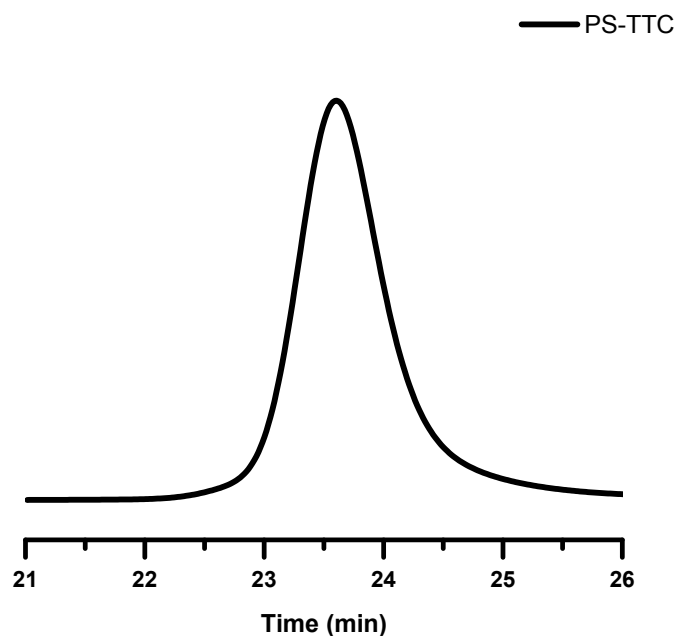


Figure S35. Normalized SEC-RI trace (THF mobile phase, 25 °C) of **PS-TTC** polystyrene homopolymer before photoinduced RAFT clipping ($M_n = 7.8\text{ kDa}$, $\text{Đ} = 1.1$) determined by conventional column calibration using PS standards.

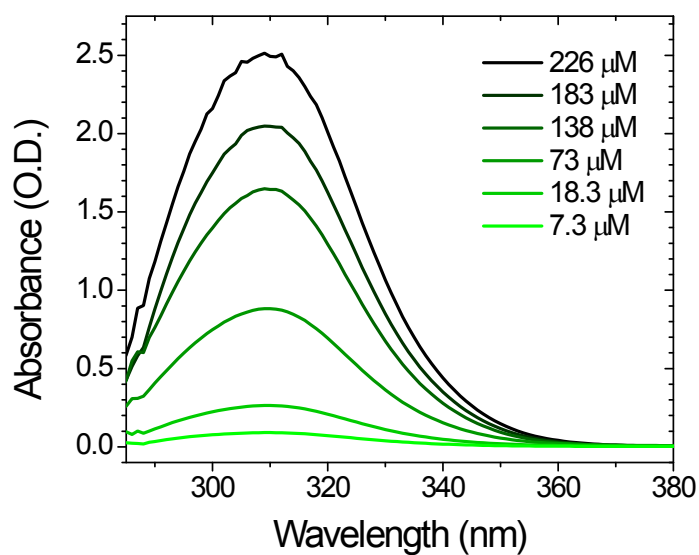


Figure S37: UV-Vis absorption of PMMA-TTC in THF at various concentrations ($\lambda_{max} = 310$ nm) diluted from initial 5.5 mM solution.

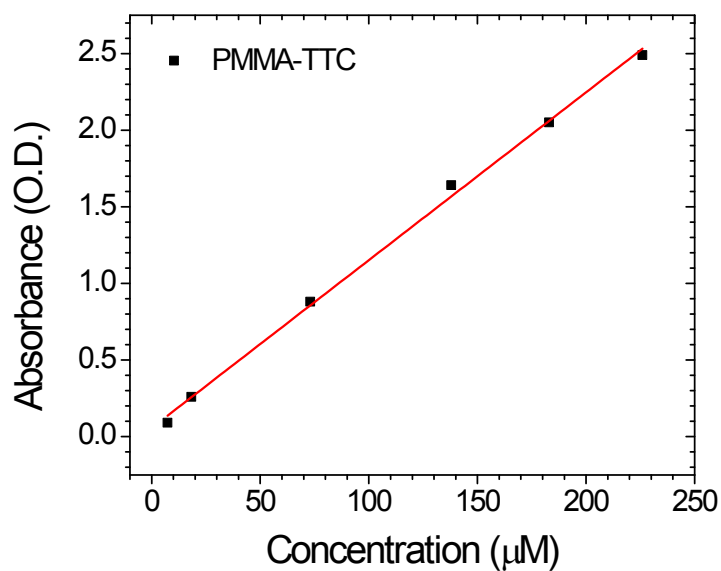


Figure S38: Absorbance vs. concentration linear calibration curve for PMMA-TTC in THF at 310 nm.

$$\text{Fit: } y = m \cdot x + b$$

Slope (m) = Molar absorptivity = $10,950 \text{ L mol}^{-1} \text{ cm}^{-1}$ (at 310 nm)

R squared = 0.9970

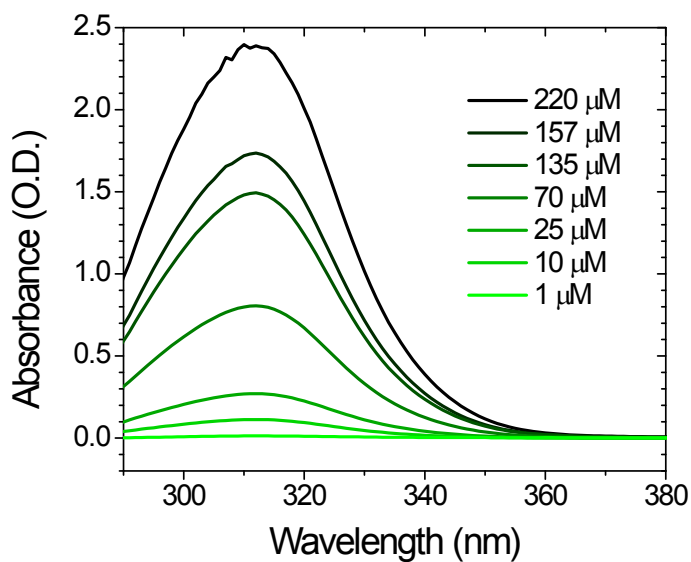


Figure S39. UV-Vis absorption of PS-TTC in THF at various concentrations ($\lambda_{max} = 312$ nm) diluted from initial 5.5 mM solution.

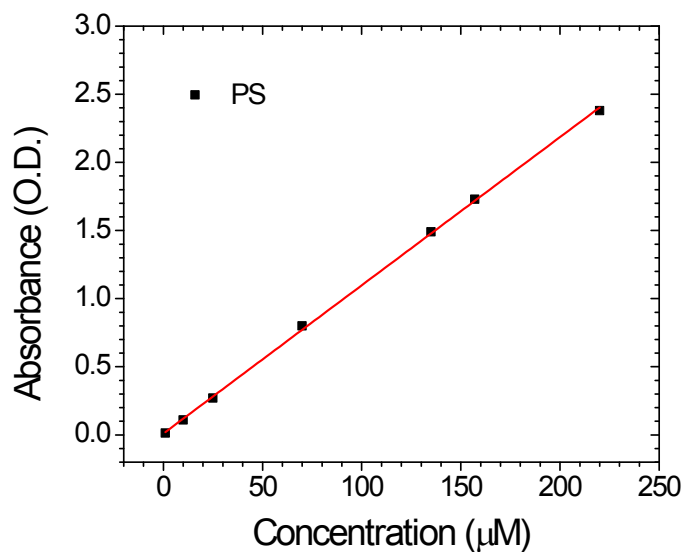


Figure S40. Absorbance vs. concentration linear calibration curve for PS-TTC in THF at 312 nm.

$$\text{Fit: } y = mx + b$$

Slope (m) = molar absorptivity = $10,880 \text{ L mol}^{-1} \text{ cm}^{-1}$ (at 312 nm);

$$R^2 = 0.9995$$

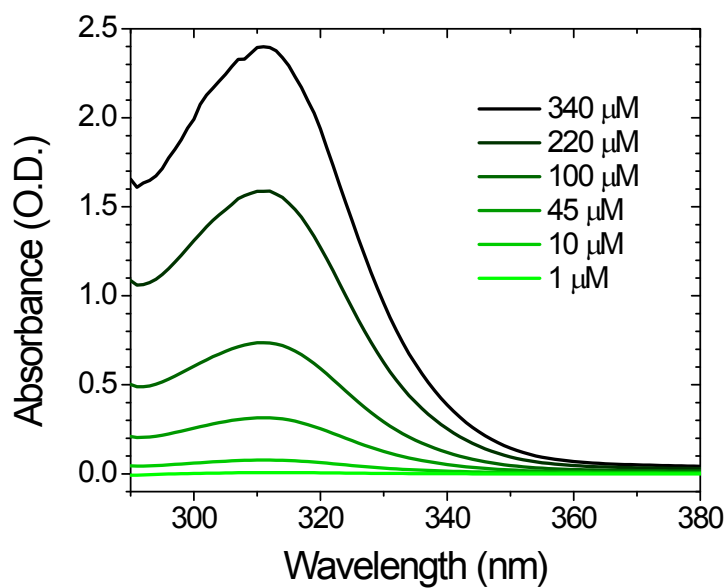


Figure S41: UV-Vis absorption of P2VP-TTC in THF at various concentrations ($\lambda_{max} = 311$ nm) diluted from initial 5.5 mM solution.

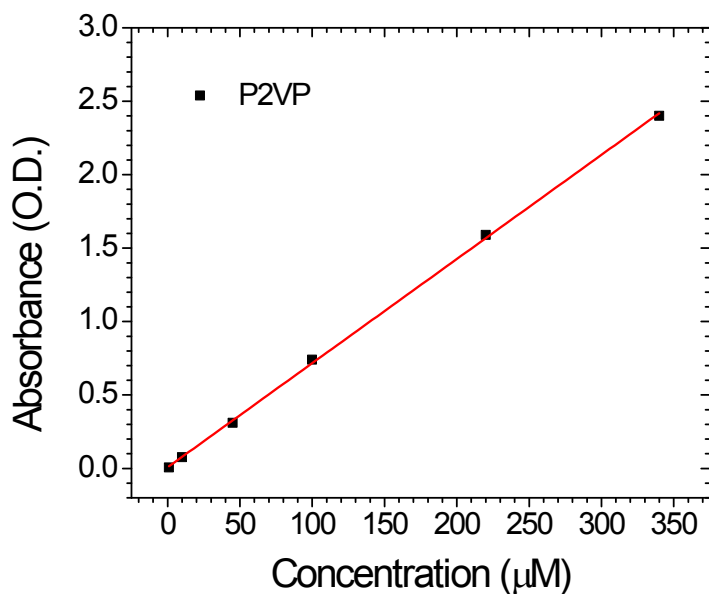


Figure S42. Absorbance vs. concentration linear calibration curve for P2VP-TTC in THF at 311 nm.

$$\text{Fit: } y = mx + b$$

Slope (m) = molar absorptivity = $7,090 \text{ L mol}^{-1} \text{ cm}^{-1}$ (at 311 nm)

$$R^2 = 0.9995$$

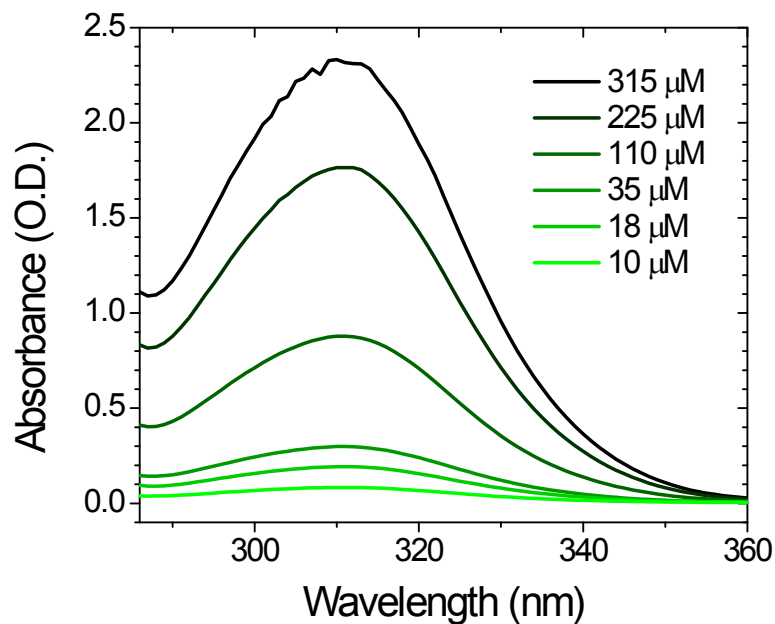


Figure S43: UV-Vis absorption of P4VP-TTC in toluene/DMAC (1:1) at various concentrations ($\lambda_{max} = 311$ nm) diluted from initial 5.5 mM solution.

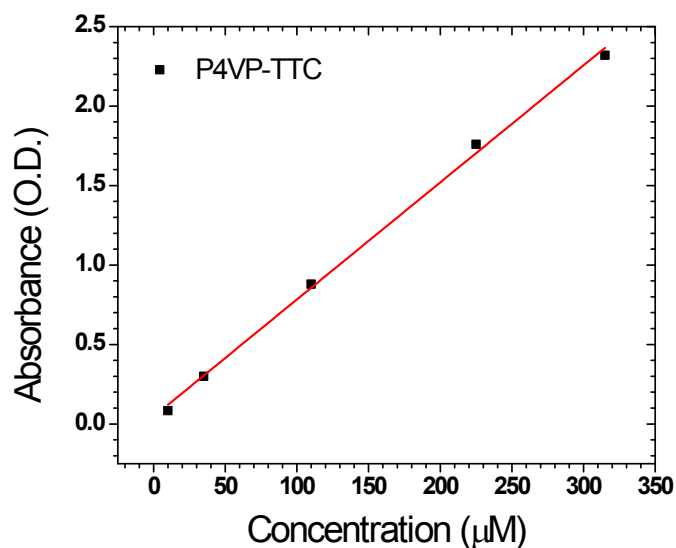


Figure S44: Absorbance vs. concentration linear calibration curve for P4VP-TTC in toluene/DMAC (1:1) at 311 nm.

$$\text{Fit: } y = m \cdot x + b$$

Slope (m) = Molar absorptivity = $7,360 \text{ L mol}^{-1} \text{ cm}^{-1}$ (at 311 nm)

$$R^2 = 0.9980$$

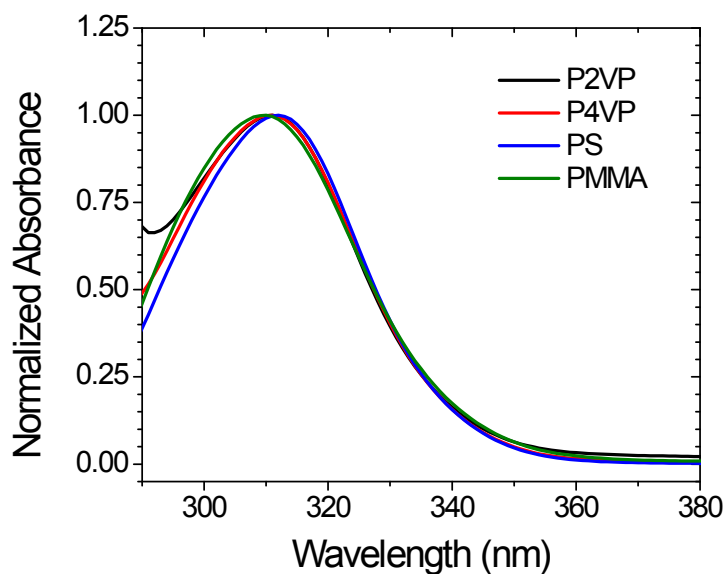


Figure S45: Normalized absorbance of TTC functionalized polymers comparing λ_{max} .

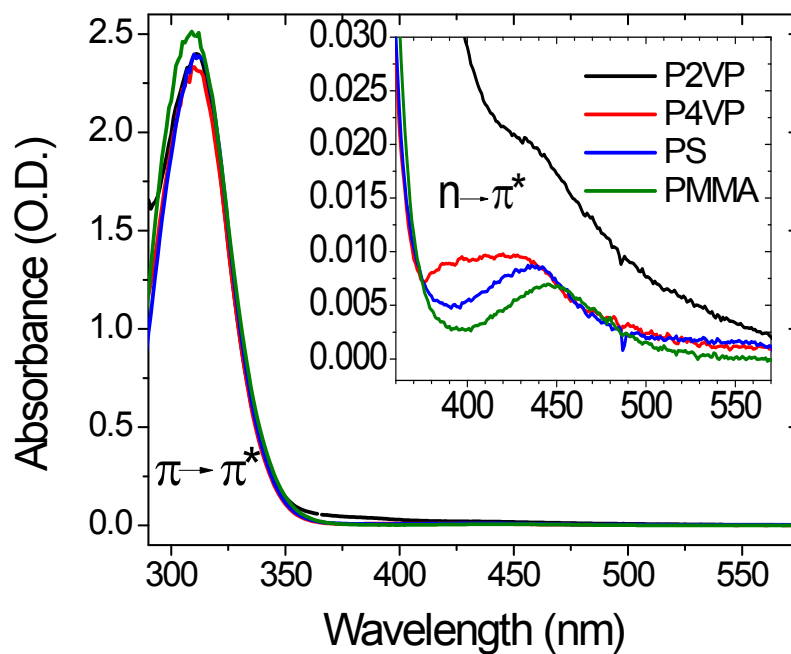


Figure S46: UV-Vis absorbance for TTC functionalized polymers with zoomed inset showing $n-\pi^*$ transition absorbance wavelength maxima.

Table S1: Comparison of λ_{max} used for kinetic experiments and molar absorptivity in $L mol^{-1} cm^{-1}$ at 365 nm and 452 nm (P2VP-TTC) for TTC functionalized polymers.

| Polymer | λ_{max} $\pi = \pi^*(nm)$ | λ_{max} $n = \pi^*(nm)$ | Molar Absorptivity (L $mol^{-1} cm^{-1}$) at 365 nm | Molar Absorptivity (L $mol^{-1} cm^{-1}$) at 452 nm |
|---------|--------------------------------------|------------------------------------|--|--|
| P2VP | 311 | 440 | 197 | 71 |
| P4VP | 311 | 420 | 76 | - |
| PS | 312 | 434 | 70 | - |
| PMMA | 310 | 445 | 173 | - |

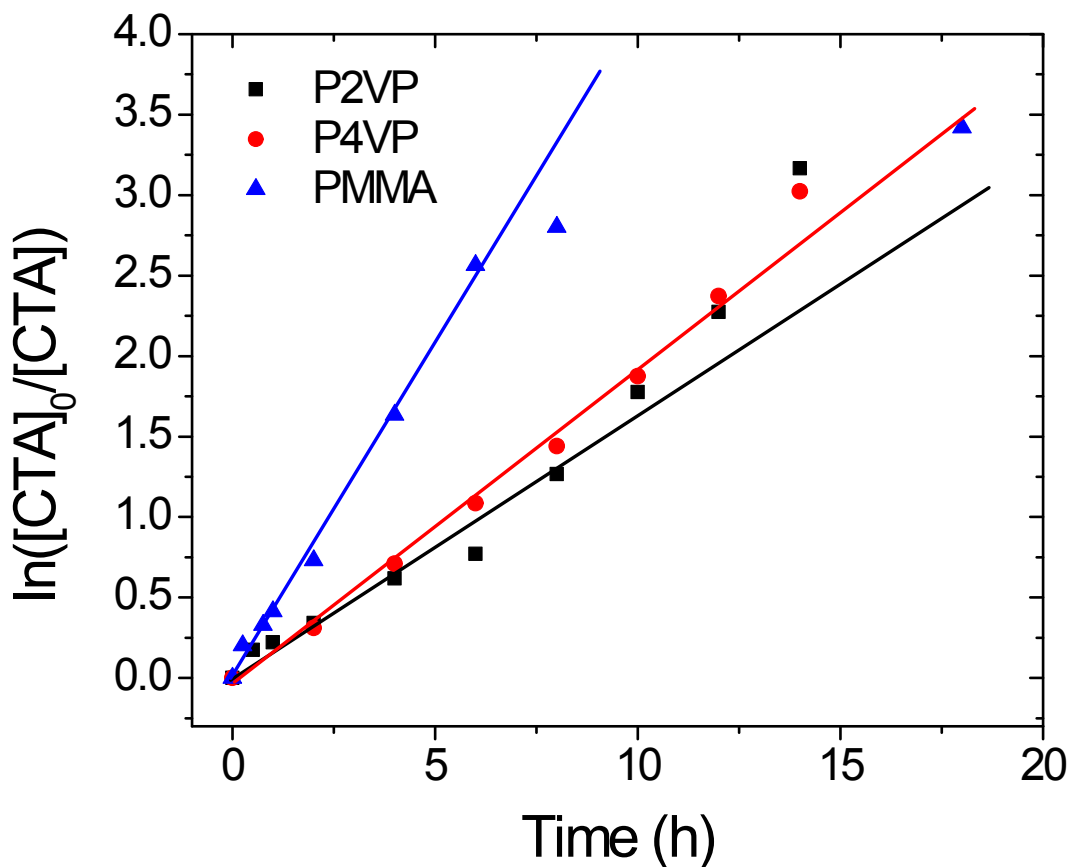


Figure S47: Logarithmic normalized concentrations of remaining CTA ($\ln[CTA]_0/[CTA]$) as a function of time (h) using EPHP (15 equiv. to CTA) in their respective reaction solvent at 28 ± 3 °C ($[CTA]_0 = 5.5$ mM) while irradiating with 365 nm light.

REFERENCES

1. Moad, G.; Chong, Y. K.; Postma, A.; Rizzardo, E.; Thang, S. H. Advances in RAFT polymerization: the synthesis of polymers with defined end-groups. *Polymer* **2005**, *46*, 8458-8468.
2. Fultz, B. A.; Terlier, T.; Dunoyer de Segonzac, B.; Verduzco, R.; Kennemur, J. G. Nanostructured Films of Oppositely Charged Domains from Self-Assembled Block Copolymers. *Macromolecules* **2020**, *53*, 5638-5648.